Effect of Static and Harmonic Loading on Honeycomb Sandwich Beam by Using Finite Element Method

Emmanuel Chukwueloka Onyibo

Submitted to the
Institute of Graduate Studies and Research
in partial fulfillment of the requirements for the degree of

Master of Science
in
Mechanical Engineering

Eastern Mediterranean University
August 2022
Gazimağusa, North Cyprus

Approval of the Institute of Graduate Studies and Research

Prof. Dr. Ali Hakan Ulusoy
Director

I certify that this thesis satisfies all the requirements as a thesis for the degree of Master of Science in Mechanical Engineering.

Assoc. Prof. Dr. Murat Özdenefe
Chair, Department of Mechanical Engineering

We certify that we have read this thesis and that in our opinion it is fully adequate in scope and quality as a thesis for the degree of Master of Science in Mechanical Engineering.

Asst. Prof. Dr. Babak Safaei
Supervisor

Examining Committee

1. Prof. Dr. Qasim Zeeshan

2. Assoc. Prof. Dr. Shaban Ismael Albrka

3. Asst. Prof. Dr. Babak Safaei

ABSTRACT

The aim of this paper is to present a proposed honeycomb core shape and compare it with normal hexagonal shape core in a sandwich beam. The sandwich cores were simulated in finite element with different materials, aluminium and epoxy-carbon with six layers are used as face sheet and the results are compared to those obtained theoretically. Simulation of 3-point bending test is performed in commercial software ANSYS to verify the analytical results with the numerical results. Hence, for simplicity one layer of the skin is used on the equivalent model of sandwich for lesser computational time and more accurate evaluation. Simulation of harmonic analysis of hexagonal core and proposed core shape was carried out in frequency domain to identify the core with less deformation under high frequency and can withstand harmful effects. The proposed core shape model having the same cell numbers and material as the normal hexagonal model is compared with experimental results, it is observed that the proposed core shape model has good flexural stiffness, resonance, fatigue, and stress resistance at a higher frequency. Lastly, the bending and critical buckling loads of a sandwich beam structure subjected to thermal load and axial compression were simulated and temperature distribution across sandwich layers was investigated by finite element analysis and validated analytically.

Keywords: Honeycomb; Sandwich; Static Analysis; Harmonic Analysis; Finite Element Method; Heat Flux.

ÖZ

Bu makalenin amacı, önerilen bir petek çekirdek şeklini sunmak ve bunu bir sandviç kirişte normal altıgen şekilli çekirdek ile karşılaştırmaktır. Sandviç çekirdekler farklı malzemelerle sonlu elemanlarda simüle edilmiş, yüzey levhası olarak alüminyum ve altı katmanlı epoksi-karbon kullanılmış ve sonuçlar teorik olarak elde edilenlerle karşılaştırılmıştır. Analitik sonuçları sayısal sonuçlarla doğrulamak için 3 noktalı eğme testinin simülasyonu, ticari ANSYS yazılımında gerçekleştirilir. Bu nedenle, basitlik için, daha az hesaplama süresi ve daha doğru değerlendirme için eşdeğer sandviç modelinde cildin bir tabakası kullanılır. Altıgen çekirdeğin harmonik analizinin simülasyonu ve önerilen çekirdek şekli, çekirdeğin yüksek frekans altında daha az deformasyonla tanımlanması ve zararlı etkilere dayanabilmesi için frekans alanında gerçekleştirilmiştir. Normal altıgen model ile aynı hücre sayılarına ve malzemeye sahip önerilen çekirdek şekli modeli deneysel sonuçlarla karşılaştırıldığında, önerilen çekirdek şekli modelinin daha yüksek bir frekansta iyi eğilme sertliği, rezonans, yorulma ve stres direncine sahip olduğu gözlenmiştir. Son olarak, termal yüke ve eksenel sıkıştırmaya maruz kalan bir sandviç kiriş yapısının eğilme ve kritik burkulma yükleri simüle edilmiş ve sandviç katmanlar arasındaki sıcaklık dağılımı sonlu eleman analizi ile incelenmiş ve analitik olarak doğrulanmıştır.

Anahtar Kelimeler: Petek Sandviç; Statik Analiz; Harmonik Analiz; Sonlu Eleman Yöntemi. Isı Akısı.

DEDICATION

TO MERCIFUL GOD AND TO MY FAMILY

ACKNOWLEDGMENT

To begin with, I praise the almighty God for this mission to be completed with joy and happy ending, irrespective of the challenges and uncertainty along the way.

I was honored to have great professors in the department that contributed to my development so far over the time. My biggest gratitude, royalty and respect to my supervisor Assistant Professor Dr. Babak Safaei, for his sacrifice, guidance and dedication towards my education life career, the impact will forever be in motion.

I am thankful to my lovely parents who gave their all till yield point to see me succeed. Thanks for all the sacrifice and support, without them there will be no me.

PREFACE

The passion has always been curiosity driven since my childhood, I have been scolded by my parent for decoupling my toy cars in quest to see what is inside and how it works. Mechanical engineering is the profession of my life by default.

I have strong passion for nature and spent so much time on ecosystem related report (Nat Geo WIlD). I realized that manufacturing is all about connecting the dot, the fastest and most flexible way is by computational means, I adopted Finite element method simulation to reduce major limitations and prepare the mind on what to expect during experimentation.

TABLE OF CONTENTS

LIST OF TABLES

LIST OF FIGURES

LIST OF ABBREVIATIONS

°C	Degrees Centigrade
2D	Two Dimensional
3D	Three Dimensional
4D	Four Dimensional
AA	Aluminium Alloy
Al	Aluminium Element
APDL	Ansys Parametric Design Language
BM	Base Metal
BMC	Bulk moulding compound
CAD	Computer Aided Design
CC	Clamped-Clamped
CF	Clamped-Free
CW	Clockwise
DOE	Design of Experiment
FEM	Finite Element Model
GPa,	Giga Pascal
HAZ	Heat-Affected Zone
HC	Honeycomb Composite
Hz	Frequency
Mm	Millimetre
MPa	Mega Pascal
PVC	Polyvinyl chloride
R&D	Research and Development

RRIM	Reinforced reaction injection moulding
RTMM	Resin Transfer Moulding Method
RVE	Representative Volume Element
SAN	Styrene Acrylonitrile
SMC	Sheet Moulding Compounds
SRIM	Structural reaction injection moulding
UC	Unit Cell

Chapter 1

INTRODUCTION

1.1 Honeycomb Structure

The honeycomb structure is a natural or man-made structure that has a honeycomb geometry to reduce the volume of material to attain minimum weight and minimal cost [1]. The geometry of honeycomb structures can vary greatly, but the typical characteristic of such structures is the sequence of hollow cells created between thin vertical walls. Honeycomb structures are widely used in almost every part of the manufacturing sector, because of their advantages, including extremely low weight/force ratios, which leads to lower weight, lower fuel usage, composite sandwich panels are used in aerospace and civil infrastructure applications because they have a higher flexural/transverse shear stiffness and, as a result, a higher corrosion resistance [2]. The cell arrangement is mostly hexagonal in section, researchers have experimented with a lot of shapes on sandwich structures, circular [3], triangular [4], square or rhombic [5], and pyramid lattice structures [6]. Honeycomb normally has a regular hexagonal geometry (the sides are equal, the angles are all 120º and the cell walls are of the same thickness) due to this, their deformations can be easily analyzed and equations of orthotropic properties are obtained [7]. Sandwich panels behaviors depend mainly on the geometric arrangement of core and facing materials [8]. Honeycomb sandwich panels normally consist of two thin face sheets or skins, lightweight thicker core, moreover, the core is made of different materials which depend on the desired mechanical properties needed. In some cases, sheet metal is

often used as a skin material. The core is bound to the skin by brazing along with the glue or metal elements. Burlayenko and Sadowski [9] Filled the honeycomb cores with foam to enhance the damage resistance and equally change the structural response of the sandwich structure, which is preferably used in waterproof, sound, and heat insulation. In addition, the sandwich core is known for low density, high compression, stiffness, and shear properties.

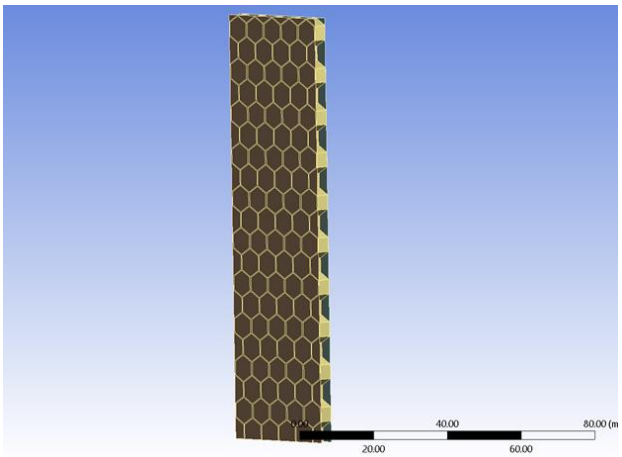

Figure 1: Honeycomb sandwich beam discrete model

Sandwich composite structures are made of two thin, rigid skin layers divided by a thicker, softer core as stated by Darzi et al. [10]. Gay and Suong [11] stated that, sandwich structures were created when two thin facings or skins were bonded or welded together on a lighter core that kept the two skins apart. The core increased the panel's bending stiffness and resistance to buckling loads [12], [13]. They also found that sandwich structures had fewer lateral deformations, more buckling resistance, and higher natural frequencies than other types of structures. Douville and Grognec [14] showed that sandwich structures were employed in a wide range of industrial applications due to their desirable combination of light weight and strong mechanical qualities. Therefore, steel is commonly used for the skins [15], [16]. Commonly used materials in the core are metallic foams and polymers [17]–[19]. Rigid-foam core is

commonly used and has moderate strength and stiffness [20]. Moreover, one of the common cores used in sandwich panels is a honeycomb [21]–[23]. In general, sandwich structures are preferred over traditional materials due to their high corrosion resistance [2] and low thermal and acoustic conductivity [24], [25]. The high thermal expansion coefficient of aluminum honeycomb sandwich constructions limits their use in thermal management systems [26]. The behavior and failure modes of sandwich structures in flexure have been observed in a variety of studies [25], [27]–[29]. A sandwich structure can fail due to a variety of damage mechanisms, including tensile failure/skin compressive [30], local skin wrinkling [31], [32], and core indentation failure [33], [34]. The sensitivity of nap-core sandwich, a unique type of structural composite with different characteristics, was studied by Marinkovic et al. [35]. Cormack et al. [36] studied the failure of sandwich beams with metallic foam cores. Ha et al. [37] studied the behaviors of nap-core sandwiches, with a particular emphasis on the effect of symmetry in nap cores.

1.1.1 Thermal Applications on Sandwich

In thermal applications, heat conduction and heat flux in sandwich beams has been experimented. Non-Fourier heat conduction was investigated in a sandwich panel with a cracked foam core by Fu et al. [38]. Under a high-temperature environment, the vibration properties of a carbon nanotube-reinforced sandwich curved shell panel were explored by Mehar and Panda [39]. Sun et al. [40] investigated the convective cooling efficiency of a sandwich panel with a hierarchical corrugated core heated from face sheets and cooled actively through the core. Onyibo and Safaei [41] applied finite element analysis to honeycomb sandwich structures. Su et al. [42] investigated the thermal insulation performance of structural insulated panels (SIPs) with glass fiber-reinforced polymer (GFRP) surfaces. Moradi-Dastjerdi and Behdinan [43] presented

a smart multifunctional sandwich plate with a central lightweight porous layer, two intermediate polymer/graphene nanocomposite layers, and two piezoceramic active faces. Zhang et al. [44] proposed an energy harvester that used an arc-shaped piezoelectric sheet to scavenge rotational energy from rotating devices. Zhao et al. [45] proposed a multifunctional carbon fiber honeycomb sandwich structure (MCFHS). Safaei et al. [46] presented an analytical solution based on molecular mechanics model to estimate the elastic critical axial buckling strain of chiral multi-walled carbon nanotubes (MWCNTs). Using experimental, theoretical, and numerical simulation methodologies, Chen et al. [47] investigated the heat transmission mechanism and thermal insulation performance of fabricated C/SiC corrugated LCSP. Safaei et al. [48] explored the thermoelastic responses of sandwich plates with porous polymeric core and proposed ultra-lightweight engineering structures of sandwich plates with one porous polymeric core and two carbon nanotube (CNT)/polymer nanocomposite outer layers. Asmael et al. [49] reviewed the ultrasonic machining of carbon fiber–reinforced plastic composites.

1.1.2 Manufacturing of Honeycomb

Manufacturing of honeycomb sandwich is majorly by corrugation, expansion, molding and, 3D printing while the most adopted manufacturing method is expansion and corrugation [50], [51]. Skin materials are laminates of glass or carbon fiber reinforced thermoplastics or mainly thermoset polymers (unsaturated polyesters, epoxies), commonly used composite is fiber-glass, carbon fiber reinforced plastic, Kevlar, and aluminum [52]. Alhijazi et al. [53] presented and analyzed the elastic properties of luffa and palm natural fiber composites (NFC) with epoxy and ecoepoxy matrixes, with the influence of fiber volume fractions taken into account. However, honeycombs are known to have four common types, aluminum honeycomb, thermoplastic

honeycomb, nomex honeycomb and stainless steel honeycomb, moreover aluminum possesses the highest strength to ratio [54]. Zaid et al. [55] concluded that the corrugated core sandwich structure has a better strength to weight ratio. The experimental eigenvalue responses of the epoxy-filled skew sandwich construction are computed for the first time by Katariya et al. [56] to demonstrate the appropriateness of equivalent type single-layer higher-order theory for the analysis (including through-thickness stretching term effect). The strength increases exponentially relative to the core thickness while the increase in weight is negligible.

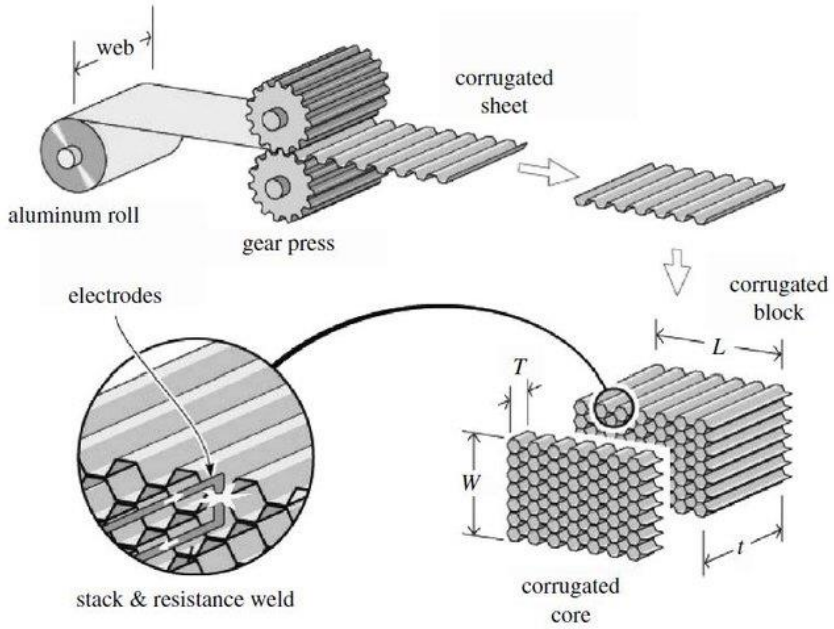

Figure 2: Honeycomb manufacturing process [57]

1.1.3 Mechanical Property of Honeycomb Structure

Mechanical property and energy absorption capability of aluminum honeycomb structures varies with impact velocity [58]. Liu et al. [59] investigated the flexural characteristics of a stiffened foam core sandwich structure. However, the honeycomb core is known for its great stiffness. Li et al. [60] stated that Sandwich composites with truss core materials have the best flexural stiffness and strength in bending

deformation, which is ideal in structural parts. Wang et al. [61] proposed a novel multilevel modeling approach for calculating Young's modulus of polymers reinforced with graphene nano-platelets. Chemami et al. [62] added orthogrid to improve the stiffness of soft honeycomb and thereby reduce the interfacial mismatch in the sandwich structure. Barbaros et al. [63] analyzed how functionally graded materials (FGMs) are prepared, manufactured, used, and their elastic properties. Li et al. [64] studied the behaviour of composite sandwich beams with glass fiber reinforced polymer (GFRP) face sheets and a balsa wood core in terms of flexural creep. Ghanati and Safaei [65] investigated the elastic buckling of regular hexagonal thin sheets made of homogeneous and isotropic materials under in-plane hydrostatic and uniaxial compression, with internal supports, translational and rotational elastic edge supports, and a mix of free, simple-support, and clamped boundary conditions. Ribeiro Faria et al. [66] investigated the dynamic behavior of sandwich beams with honeycomb cores loaded with magnetorheological (MR) gels and composite material skins under the effect of vibrations. Hence, under various forms of mechanical loads, the static deflection, frequency, and transient responses of the multilayer sandwich shell (flat/curved) structure were estimated by Katariya and Panda [67]. Fazilati et al. [68] showed, honeycomb structures are commonly used as energy shock absorbers due to their strong crashworthiness characteristics of high energy absorption potential and high strength-to-weight ratio. Ha et al. [69] presented the nap-core sandwich's fabrication, characteristics, and uses, with a focus on the sandwich's sensitivity and a special focus on the effect of symmetry in nap cores [37]. Lu et al. [70] compared Nomex and aluminum with sandwiches made from carbon fiber/epoxy and concluded that the bending strength of carbon fiber/epoxy honeycomb is greater. Choosing the best honeycomb core for your application can be a very major factor. Hence, not only

mechanical property strengths and stiffness, but also the problem of the environment must also be considered. In order to study and observe the low velocity impact energy response of sandwich structures used for railways, Sakly et al. [71] introduced finite element method, to simulate ballast impacts, a high-speed and low weight test bench was designed. The graded sandwich shell structure's thermal eigenvalue responses are numerically assessed under varied thermal loadings while considering temperature-dependent characteristics as investigated by Sahoo et al. [72]. He et al. [73] Carried out experimentally and numerically, the low velocity effect of CFRP face sheets and aluminum alloy cores. However, many researchers used carbon fiber as skin [74]. It comes in two weaves, unidirectional (all fibers are parallel) and bidirectional (fibers cross at a 90-degree angle). Furthermore, recently many researchers carried out experiments on 3D printed cores [60], [75]–[77].

Table 1: Material properties of aluminum [78]

Material property	Value
Density	2700 kg/m^3
Young's Modulus	71070 MPa
Yield Strength	268 MPa
Compressive Strength	2.5 MPa
Compressive Modulus	540 Mpa
Tensile Strength	367 Mpa

1.2 Definition of Problem

The response of honeycomb structures under static loading with different cores, aluminum, honeycomb, and SAN foam with the same face sheet will be investigated in this study, in view of modal analysis and static structure. In order to find the most

influenced output like equivalent stress, stiffness and natural frequency, the design of the experiment and parameter correlation was used in the ANSYS tool for understanding the parametric response. Lastly, harmonic analysis of two different shaped geometry cores are investigated and stresses reviewed at their peak frequencies.

1.3 Need for Research

Honeycomb sandwich is really one of the fundamentals to make a composite strong, stiff, very light, safe and have wonderful performance. Honeycomb materials are majorly used where high strength to weight ratio, stiffness to weight core which can take many shapes, the common is hexagonal shape. The core handles shear load, while the skins resist compression and tension. This paper aims to guide the design of honeycomb sandwich structures done with finite element analysis software. The characteristic of honeycomb at microstructure and unit cell will be discussed Moreover, much demand on light weight honeycomb structures that can withstand heavy loads under different working condition are on high demand. Experimental approach can be time consuming and costly, this created room for massive research using FEA on loading response with various cores and thickness, in order to investigate the mechanical properties.

1.4 Objectives of Study

This paper aims to investigate the static loading effect on Sandwich beam, its flexural stresses were clearly analyzed and harmonic analysis of the two core shapes was investigated, the amplitude of the response, phase angle and corresponding stresses was detailed. Epoxy carbon UD (230GPa) was used as face skin, aluminum, honeycomb and SAN foam materials used as core. In addition to that, the aluminum alloy was later used as face skin while maintaining honeycomb as the core for validation. The ANSYS finite element method (FEM) simulation results were

validated analytically and it is in accordance with the stiffness of the sandwich beams equation. The natural frequency of honeycomb core and mode shapes were illustrated. In order to gain more insight into certain systems' deformation mechanisms, ANSYS is used as the finite element simulation and comparisons between both honeycomb cores materials deformation, stress resistance and mode shapes. Lastly, improved flexural stiffness, resonance resistance and optimization check between the normal hexagonal honeycomb core and proposed shape core are confirmed.

Chapter 2

LITERATURE REVIEW

2.1 Representative Volume Element (RVE) and Homogenization

RVE is a volume that statistically reflects a composite. That is volume that effectively includes a sampling of all microstructural heterogeneities (inclusions, fibers, voids, grains, etc.) that occur in the composite. Furthermore, hexagonal honeycomb consists of a 'unit cell' repeated many times in one or more spatial directions. This unit cell is usually a fraction of the size of the overall structure under investigation. Hence, in ANSYS Workbench a new feature called "Material Designer" has been introduced. An RVE is a material volume with a representative effective behavior of the entire material as defined by Aboudi et al. [79]. Bargmann et al. [80] generated 3D RVEs for a broad class of materials. Babu et al. [81] used RVE to create microstructure of short fiber, which are efficient in predicting the stiffness of the short fiber composites.

In honeycomb finite element modelling, the representative volume element was used to transform a honeycomb structure into a homogeneous and orthotropic substance through homogenization technique as proposed by Sorohan et al. [82]. Safaei et al. [83] carried out symmetric boundary conditions of platelet reinforced, allied unit cell model using ANSYS. Actually, different tools are used to evaluate honeycomb's RVE, such as Easy PBC in ABAQUS and material designer in ANSYS. These methods need material properties, fiber and volume division as inputs, RVE dimensions, the most convenient mesh size and form can be specified automatically and finally the RVE

model can be solved. Qiu et al. [84] predicted the effective elastic characteristics of honeycomb structures using a computational homogenization approach (CHT) based on the finite element method (FEM). Figure 3 depicts the representative volume element (RVE) of honeycomb core.

In order to compute the stresses in a system, the FEM is also used to explore a honeycomb core, due to the complex geometry an enormous number of elements are required, this vast number of elements makes calculation times exponentially increase as far as analyzing a major structure is concerned. However, simulating a million-unit cell lattice of volumetric elements or shell elements, it will be computational expensive. Hence, homogenization takes a unit cell and characterizes how it will behave in isolation, thereby indicating the stiffness matrix of the material. The number of elements can be significantly reduced by replacing the honeycomb core with a homogeneous core with orthotropic properties as shown Figure 4. The same rigidity as the wobbly center must be the homogeneous core. Wahl et al. [85] carried out finite element simulation with a homogenized core calculating the shear stresses in the honeycomb core. Homogenization of the cellular structure to optimize the structure of the cellular structure [86].

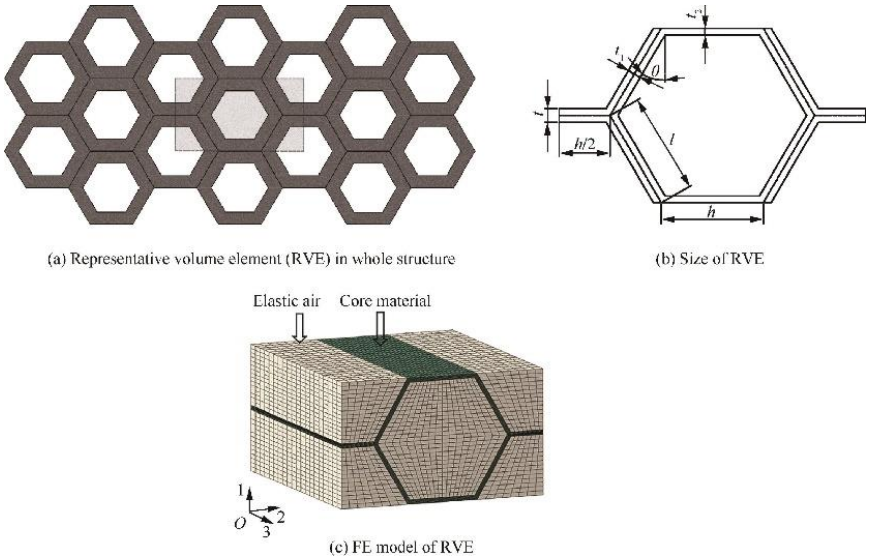

Figure 3: Representative volume element (RVE) (a) whole structure; (b) size of RVE; (c) FE of RVE [84]

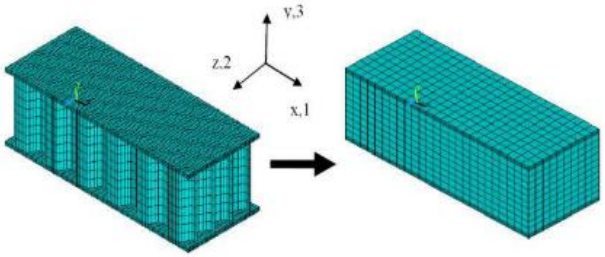

Figure 4: FE model of honeycomb and equivalent core [86]

2.1.1 Finite Element Analysis (FEA)

Engineers invented the finite element method (FEM), which is a computational approach/technique for obtaining an approximate solution to engineering problems. FEA is efficient, time saving and less expensive. A measurement model that divides the structure into a number of minor subdivisions replaces the overall framework structure under evaluation (finite elements). If the mechanical problem is defined by a differential equation, the equation must be translated into a variational formulation (Galerkin method, mixed methods, discontinuous Galerkin method and many others), a discretization approach, one or more solution algorithms, and post-processing techniques define a finite element method. Moreover, finite element analysis (FEA) is

used to check the correctness of theoretical predictions and compare them to experimental outcomes of structures. The computational method of finite element analysis (FEA) is used to predict how a product will react to forces, vibrations, heat, fluid movement, and other physical influences in the real world. Finite element analysis (FEA) is used to solve problems in a variety of fields, including heat transmission, vibrations, material strength, acoustics, and many more. In addition, to solve problems relating to domains in FEA, finite element methods (FEM) are applied and it include the galerkin method, weighted residual approach, and different numerical integration methods. It is entirely a mathematical method. Yang et al. (B. Yang et al., 2021) used FEA to simulate intra-laminar and inter-laminar delamination of the CFRP face sheets, as well as adhesive and honeycomb core failure. Hussain et al. [8] modeled the honeycomb sandwich structure using ANSYS, a commercially accessible finite element tool, and fatigue simulations were performed to evaluate specimen life under load-displacement response. Harland et al. [87] developed a computational 3D FEA model to examine the nonlinear mechanical behavior of the re-entrant core under load. To investigate the dynamic deformation evolution of two face sheets and an auxetic reentrant honeycomb core, Xiao et al. [88] developed a finite element (FE) model. Kumar and Patel [89] calculated the dynamic response of the sandwich panel using the ABAQUS finite element modeling program, determining the structural behavior of honeycomb sandwich panels when subjected to blast loading on various cores (octagonal and square structures). Adams et al.[90] conducted finite element simulation to study the reaction of an elastomeric pre-buckled honeycomb structure under impact loads in order to determine its suitability for use in helmet liners. In general, every engineering discipline uses Finite Element Analysis, including

aerospace, automotive, biomedical, chemicals, electronics, energy, geotechnical, biomedical, chemicals, manufacturing, and polymers industries.

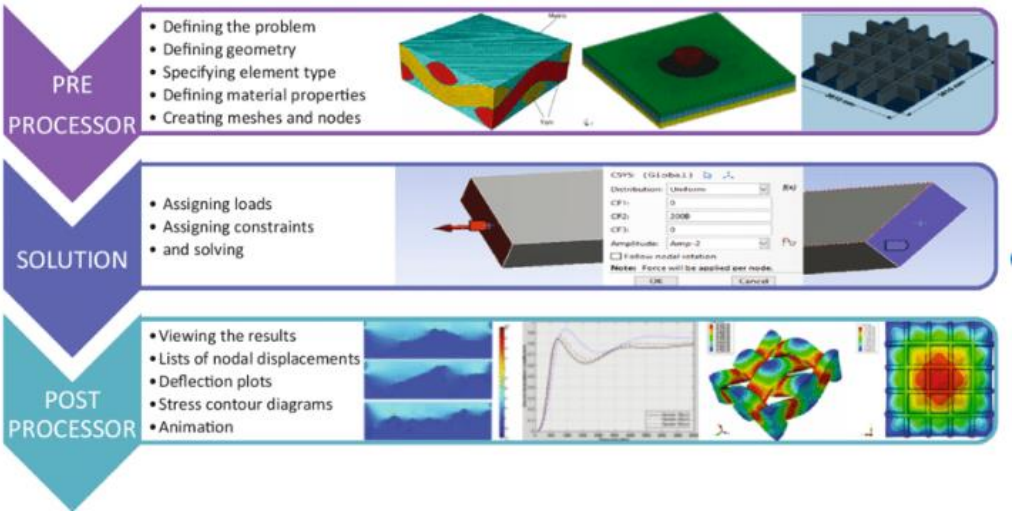

Figure 5: Overview of FEA adapted from [91]

2.1.2 FEA of Honeycomb

Numerical tools used for differentiating and discretization (meshing) of geometries as shown in Figure 6. In modelling and simulation, variety of method are used to predict range of properties, namely, mechanical properties, thermal analysis, structural analysis, buckling analysis and stiffness. Xie et al. [92] investigated mechanical properties of combined structures of stacked multilayer Nomex honeycombs, established the finite element model of Nomex honeycombs and compared with experimental data. In-plane and out-of-plane crushing properties of the honeycomb core. According Sorohan et al. [82] to , the out-of-plane orientation of the core was discovered to be the strongest, absorbing a large amount of energy during deformation. The meshing employed by researchers for analysis is depicted in Table 2.

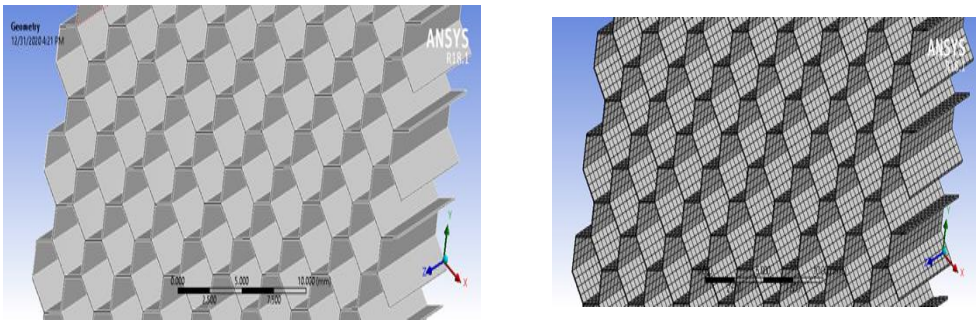

(a) (b)

Figure 6: Meshing (a) actual model (b) finite element model [93]

Table 2: Meshing of honeycomb

Element type	**Nodes**	**Elements**	**Ref.**
Polygonal mesh	630	314	[94]
SOLID186	6750		[95]
185-node	11,220	5000	[96]

Since the development of FEA in the aerospace industry in the 1950s by Boeing and Bell Aerospace in the United States and Rolls Royce in the United Kingdom. The first papers was published by M.J. Turner, R.W, since then it became an essential engineering tool. A lot of FEA Software's have been developed. Table 3 depicted the major FEA software's used and their companies.

Table 3: FEA software's and developer

Software	**Developer**	**Platform**
Mathematica	Wolfram Research	Linux, Mac OS X, Windows, Raspbian, Online service.
LS-DYNA	LSTC-Livermore Software Technology Corporation	Linux, Windows
MATLAB	MathWorks	Linux, Mac OS X, Windows
CosmosWorks	Dassault systemes solidworks corp.	Windows
Autodesk Simulation	Autodesk	Windows
ANSYS	Ansys Inc.	Windows, Linux
ABAQUS	Abaqus Inc.	Linux, Windows
Open FOAM	The OpenFOAM Foundation	Linux, Mac OS, and Windows
COMSOL	COMSOL Inc.	Windows, Mac, Linux

ANSYS and ABAQUS is the most used based on the graphic user interface (GUI), Moreover, component can be shared between most of the software, which makes FEA interesting. In the automotive sector, ABAQUS has greater penetration, while ANSYS is favored in the energy sector. ABAQUS has no room for SI unit, hence it requires a lot of focus and attention while ANSYS is flexible and lucid. ANSYS provides fine-sweep meshing and automated meshing (hexa-dominant, swept hex, hex-core, tetrahedral, and surface meshing) as investigated by Meyghani et al. [97].

The load application, depends on the analysis form of honeycomb sandwich (static load, dynamic load, fatigue load, thermal load, and buckling load). The direction and velocity of loading defines on the kind of mechanical loading involved. Atiqah et al. [98] carried out hardness properties of honeycomb natural fiber reinforcement using Izod impact and Brinell hardness tester. Using commercial finite element software, the impact response of honeycomb sandwich structures was investigated., Dai et al. [99] investigated honeycomb sandwich structures using single and repeated impact testing.

2.1.3 Optimization and Design of Experiment on Sandwich Structures

Several optimization methods are applied to find the right parameters or the optimum value of a given property (strength, stiffness) in honeycomb sandwich structures. [100] performed an experimentation on the angle of the Abrasive water jet (AWJ) aluminum honeycomb, design philosophy of Taguchi was implemented. An analysis of thin-walled steel structure and aluminum honeycomb energy absorption potential was performed by Yang et al. [101] using analysis of variance to investigate the impact of dispersed honeycomb intensity on crashworthiness indicators at four levels. ANSYS has an inbuilt program for design of experiment and optimization which saves time significantly, for instance, parameter feature connects input and outputs to the parameter interface in the workbench project. Dutra et al. [102] carried out design of

experiment on five parameters with different levels, in order to determine the essential material to change orientation, add or remove, for effective flexural strength and optimization as shown in Table 4. Moreover, design of experiment is a major step for researcher that guides directly to the desired design output. Figure 7 shows geometric factors of the honeycomb core.

Table 4: Parametric conditions for the FE model [102]

Geometric factors	Levels			
Height of cell [mm]	5	10	20	30
Honeycomb geometry	Hexagon		Rectangular	
Cells per honeycomb	42	84		126
Web thickness [mm]	1	2		3
Facing thickness [mm]	1		2	

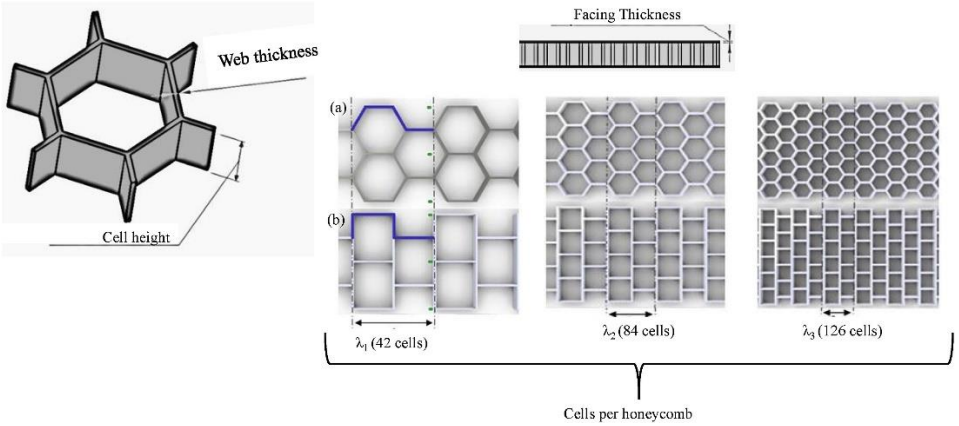

Figure 7: Geometric factors of the honeycomb core composite sandwich [102]

The metal composite material (MCM) is a type of sandwich formed in a continuous process by means of controlled pressure, heat and stress, from two thin metal skins attached to the plastic foundation. Hence, their classification regarding the core form and the support of the skin, it is possible to classify sandwich structures into the following groups: homogeneously supported, locally supported, regionally supported, unidirectional supported, and bidirectional supported as defined by Vijaya Ramnath et al. [103]

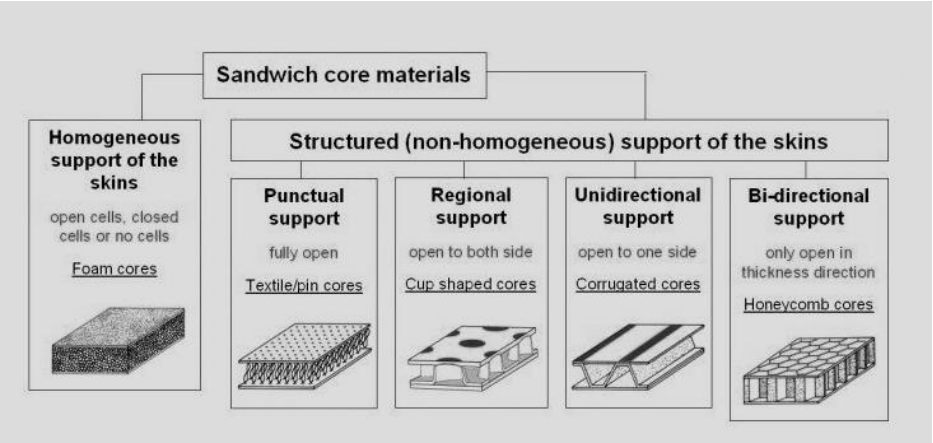

Figure 8: Classification of sandwich core [104]

Chapter 3

METHODOLOGY

3.1 Geometry and Material Properties

The honeycomb core model was created using commercial Solidworks software (IGS file format) Figure 9(a) and imported to ANSYS workbench for assembling in static structural. ANSYS Composite PrepPost (ACP) was used for the design of the face sheet, combining laminate layup from a composite material as shown in Figure 9(b). In addition, the honeycomb core was bounded on both sides by two face sheet (epoxy carbon 230 UD) as depicted in Figure 10. Lastly, Figure 11 depicts the proposed honeycomb model design.

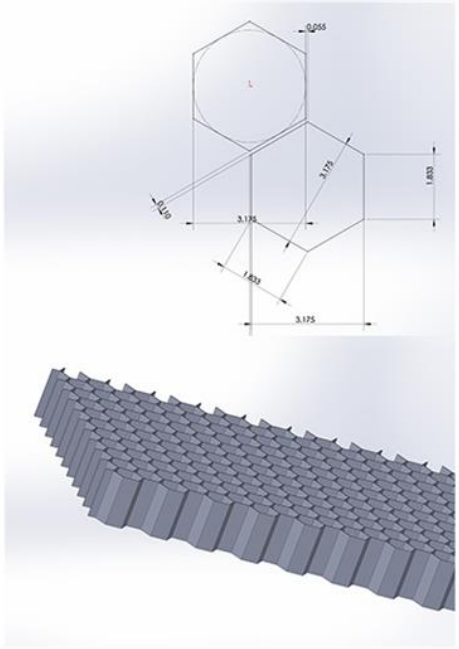

(a)

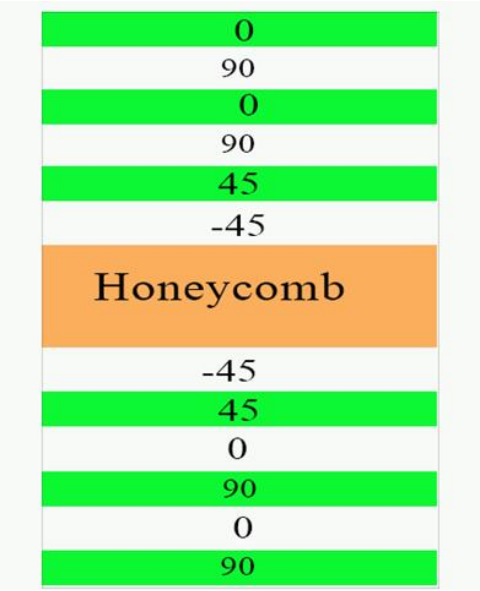

(b)

Figure 9: Schematic of honeycomb sandwich structure;(a) hexagonal honeycomb;(b) laminate layup composite

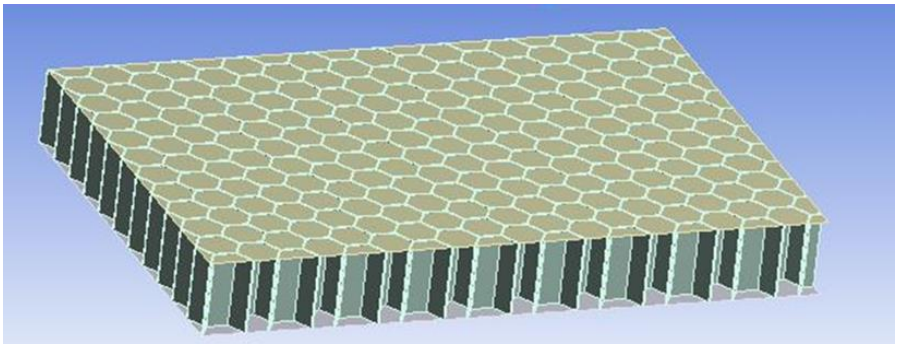

Figure 10: Bounded surface of honeycomb core and face sheet

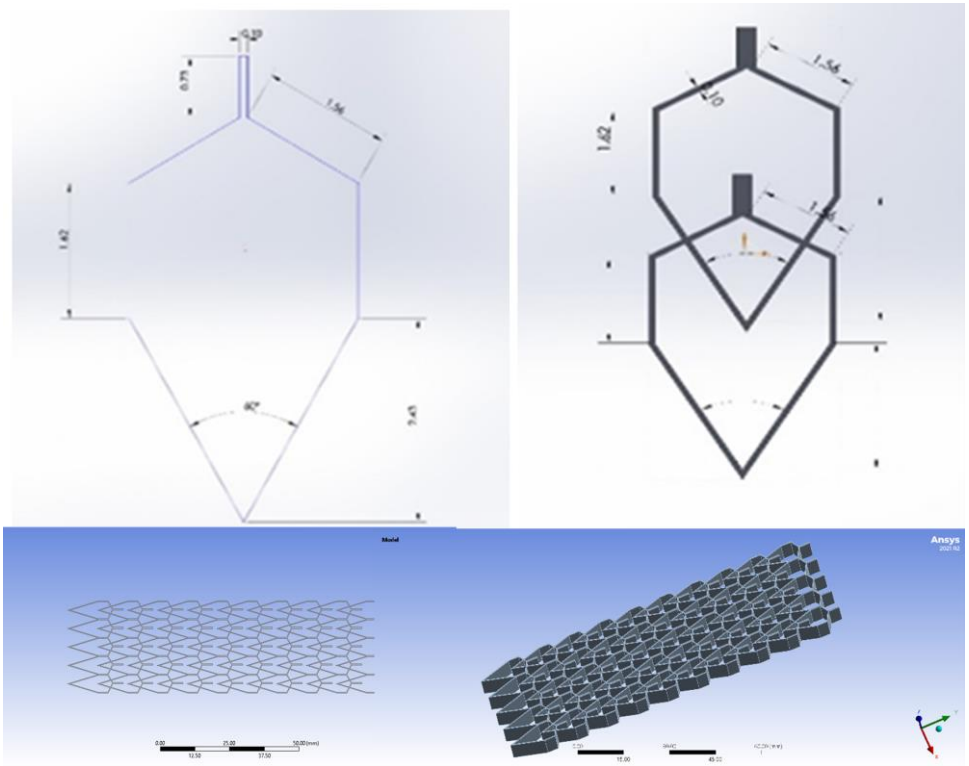

Figure 11: Proposed core honeycomb inclined edge model

3.2 Material Properties

Epoxy provides a solid, durable framework with good carbon fiber adhesion. Pre-preg is a polymer consisting of "pre-impregnated" fibers. Unidirectional (UD) carbon fiber has high bending power in a 0-degree orientation associated with the fibers against the progression of forces, Same configuration of the core was used for an isotropic solid sandwich made of epoxy carbon (thickness = 0.2 x 5mm). The lay ups used for orthotropic face sheets were [0/0/0/0/0], therefore the laminate thickness is 1mm on each skin. Table 5 listed the material properties that were used in the sandwich beam structure analysis. Aluminum, honeycomb, and SAN foam were used as the core in bending stress analysis, epoxy carbon UD (230 GPa) PrePreg was used for the face sheet. Lastly aluminum alloy and honeycomb were used as skin and core respectively for analytical validation.

Table 5: Material properties used for skin and core

Material	**Young's Modulus *E* (MPa)**	**Poisson's Ratio *v***	**Shear Modulus *G* (MPa)**	**Density *ρ* (kg/m^3)**
SAN Foam	85	0.3	32.692	103
Aluminum	7100	0.33	2669	2770
Epoxy Carbon	121000	0.27	4700	1490
Honeycomb	1	0.49	1E-06	80
Resin Epoxy	3780	0.35	1400	1160

In addition, for thermal analysis Table 6 summarizes the depicted material properties carbon fiber-polyimide was used as face sheet and carbon foam was used as the core to analyze flexural strength in cantilever beam conditions and investigate strength along the axis (buckling). Furthermore, the sandwich beam with the same material was subjected to thermal loads and the results with and without aerogel were evaluated.

Table 6: Material properties of sandwich beam for thermal analysis

Material	**Young's Modulus *E* (MPa)**	**Poisson's Ratio *v***	**Shear Modulus *G* (MPa)**	**Density *ρ* (Kg/m^3)**	**Thermal conductivity (W/m°C)**
Carbon fiber-polyimide	70000	0.36	25735	1410	2.16
Carbon foam	123.79	0.33	46538	2267	0.11
Silica Aerogel	5	0.2	20833	105	0.016

3.2.1 Meshing of Finite Element

Meshing is a method of transforming geometrical bodies into finite element entities. In this design of the sandwich structure, 8 nodded brick elements are used. In order to divide the domain into discrete elements, and to solve the equilibrium equation for each nodal location, the SOLID168 element type was used, these are high order

element that gives sufficient bending properties for this work. SOLID168 is an explicit dynamical element in a higher order, 3-D 10-node. It is ideal to model irregular meshes, for example those created from different CAD/CAM systems. The element is defined with a total of 10 nodes, each with three degrees of freedom: node x, y and z. Fine meshing is performed to take account of the transition of tension between the core material and the face sheet, as seen in Figure 12. Pham used different types of meshing methods and sizing [105]. Moreover, meshing can affect the output results, in order to be close to the Analytical solution, fine meshing was adopted for the face sheet and program-controlled mesh for the honeycomb core. The number of nodes and elements used for both face skin and honeycomb core are shown in Table 7. However, the higher the nodes and elements the longer computational time, but better the results, when compared to the exact solution.

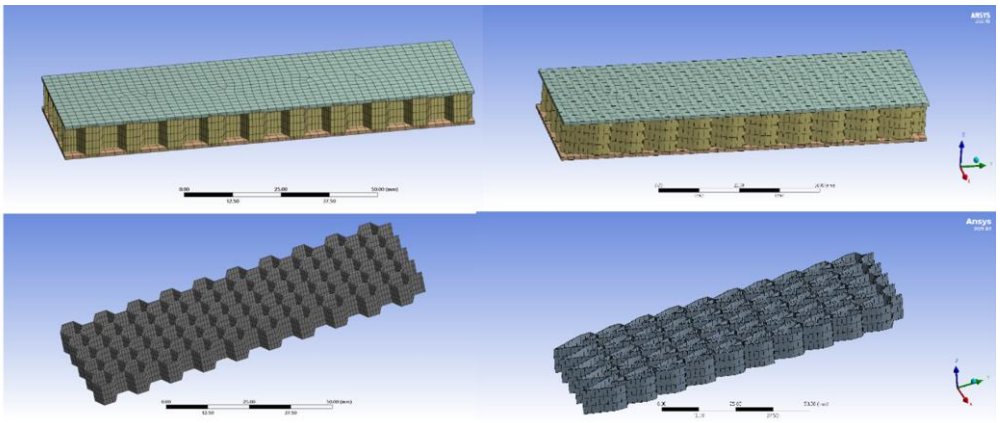

Figure 12: Finite element meshing

Table 7: Number of nodes and elements

Name	Material	Nodes	Elements	Thickness (mm)
Face-sheet	Epoxy Carbon	868	803	1
Hexagonal honeycomb core	Aluminum alloy	42469	5680	10
Proposed core	Aluminum alloy	45787	6750	10

3.2.2 Boundary Conditions and Loads

Honeycomb sandwich structure has been assigned fixed support in one end, displacement in the other end in a line of Z-axis (Horizontal to the sandwich), hence in order to mimic simply supported beam conditions, the top face skin was loaded with uniformly force in the static structural analysis of ANSYS workbench as shown in Figure 13 and Figure 14 for the hexagonal and proposed sandwich structure respectively. Figure 15 and Figure 16 analysis were carried out to investigate the modal frequencies and harmonic response, therefore treating the honeycomb core as a cantilever beam (one end fixed). Lastly, as shown in Figure 17 concentrated loading of 3-point bending test of equivalent shell model of the sandwich structure was performed to validate the analytical calculation with the simulation method.

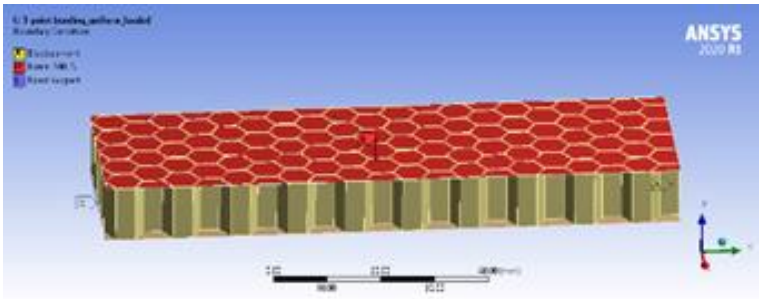

Figure 13: Loads and boundary condition of static analysis of normal hexagonal honeycomb sandwich beam.

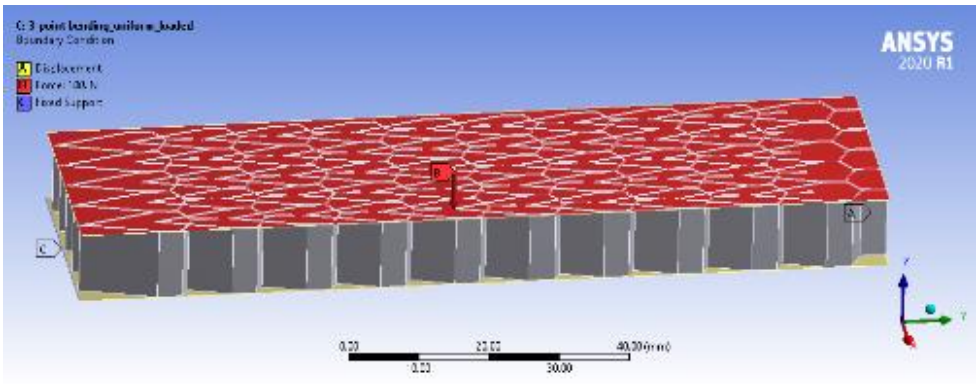

Figure 14: Loads and boundary condition of static analysis of proposed honeycomb core sandwich beam

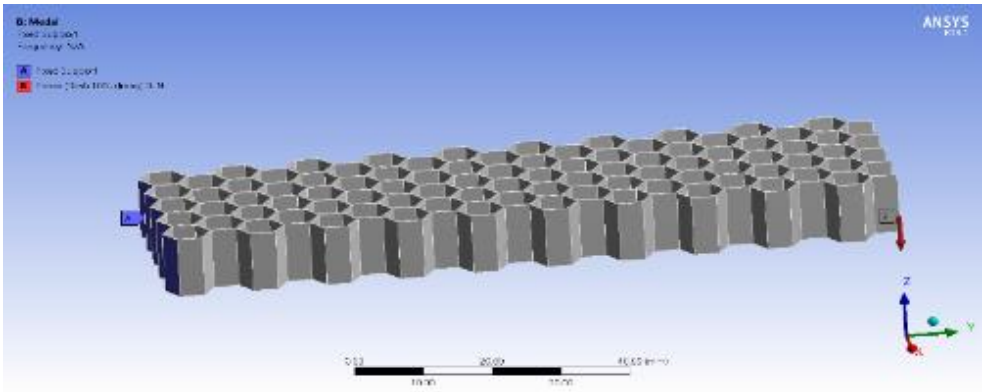

Figure 15: Harmonic response boundary condition of honeycomb hexagonal core.

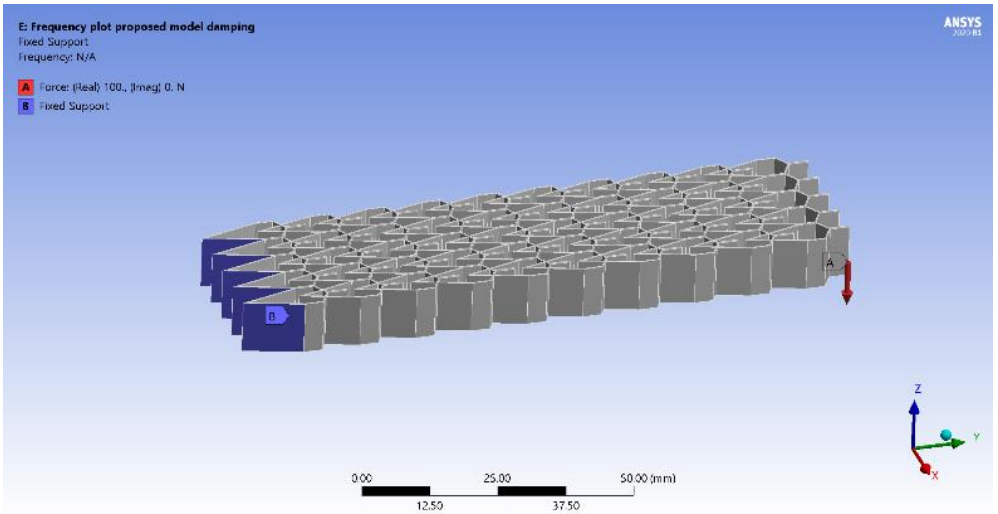

Figure 16: Harmonic response boundary condition of proposed honeycomb core.

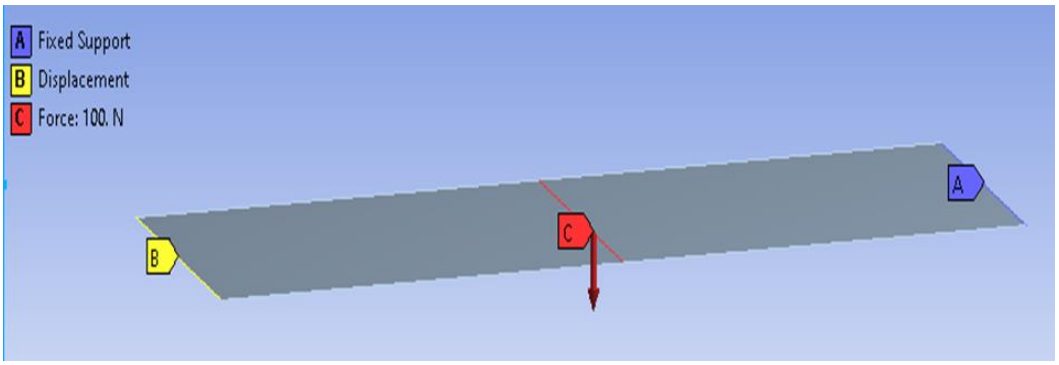

Figure 17: 3-point bending test of sandwich and boundary condition of equivalent shell model of honeycomb sandwich structure.

Axial load case was considered in sandwich buckling while point load was applied in bending tests of sandwich. However, for the buckling of sandwich beam structures, simply supported (pinned at both ends) conditions were used which could only move laterally, and in bending tests, sandwich structures were treated as cantilever Beams (fixed at one end and point load on the other end), as shown in Figure 18. In buckling, no displacement along z-direction, completely fixed on one side and moving on the other side along the direction of applied force, in this case x-direction, as shown in Figure 19. Figure 20 depicts thermal boundary conditions (high temperature applied on top skin and room temperature set at bottom skin). Finally, Figure 21 shows thermal boundary conditions for the temperature that could buckle the sandwich beam.

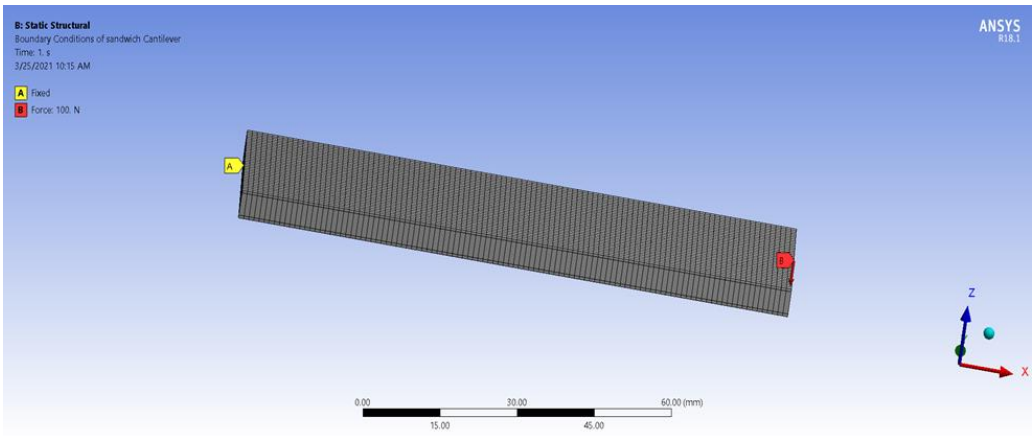

Figure 18: Cantilever for bending analysis

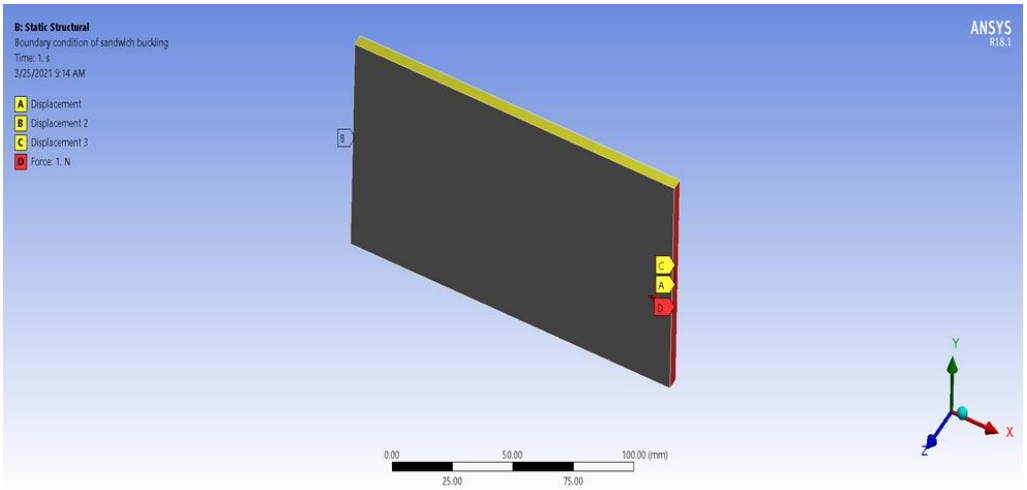

Figure 19: Simply supported, moving along horizontal direction

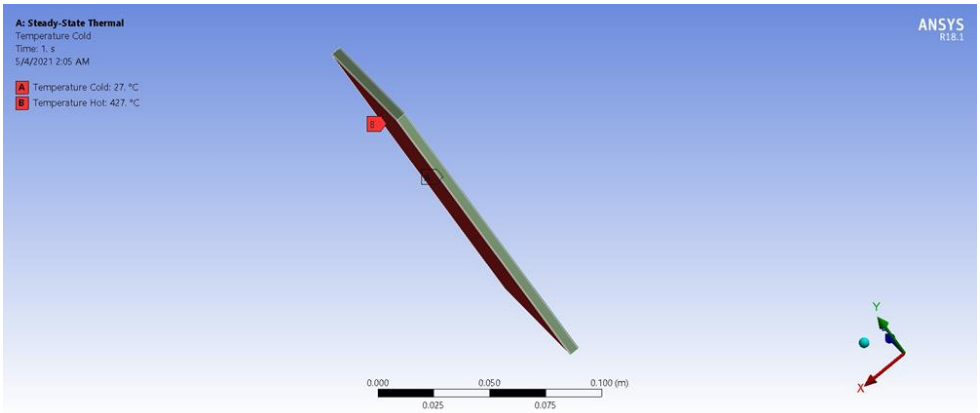

Figure 20: Steady-state temperature boundary condition (higher temperature applied on top skin

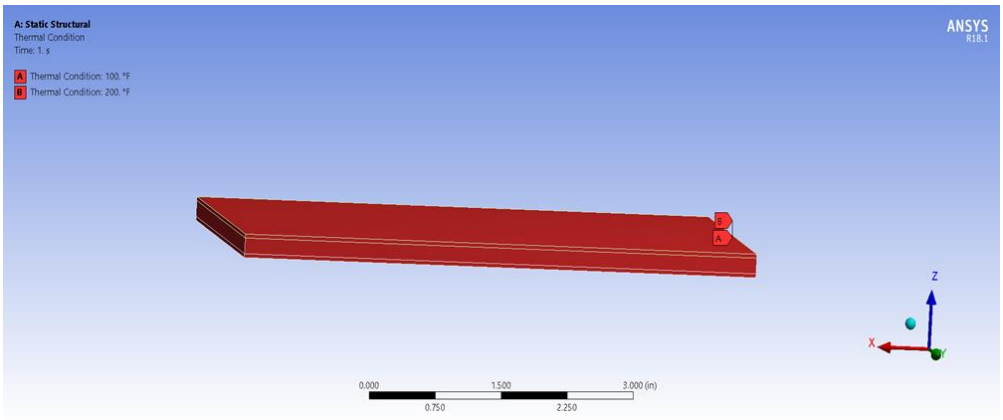

Figure 21: Thermal expansion of sandwich beam

3.3 Theoretical Analysis Sandwich Beam

The sandwich beam is made up of two thin skins with a thickness of t and a core with a thickness of c as shown in Figure 22. The overall depth of the beam is h and the width is b. The distance between the center lines of the upper and lower faces is d. D is the flexural stiffness of the sandwich beam calculated by the following equation:

$$D = E_f \cdot \frac{bt^3}{6} + E_f \cdot \frac{btd^2}{2} + E_c \cdot \frac{bc^3}{12} \quad (1)$$

where E_f and E_c are the elastic modulus of the face and core, respectively.

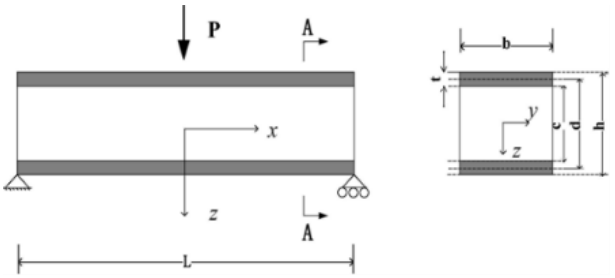

Figure 22: Sandwich beam schematic model in three-point bending

The honeycomb core's elastic modulus is significantly lower than that of the face sheet. The face is only 0.5 mm thick, significantly thinner than the core, which measures 4 mm in height. The following equations are met:

$$3\left(\frac{d}{t}\right)^2 > 100{,}6\frac{E_f}{E_c}\frac{t}{c}\left(\frac{d}{c}\right)^2 > 100 \quad (2)$$

As a result, the first and third terms of Eq. (1) can be omitted [106]. Therefore, the total flexural stiffness supplied by the faces around the sandwich's centroid axis is determined as

$$D = E_f \cdot \frac{btd^2}{2} \quad (3)$$

When the sandwich beam is loaded by central point force *P*, according to the standard sandwich beam theory [106] , the usual stress on the face is at *x = L/2*,

$$\sigma_f = \frac{PLz}{4D}E_f \left(\frac{c}{2} \leqslant z \leqslant \frac{h}{2}, -\frac{h}{2} \leqslant z \leqslant -\frac{c}{2}\right) \quad (4)$$

The shear stress in the honeycomb core is

$$\tau_c = \frac{P}{2bd}\left(-\frac{c}{2} \leqslant z \leqslant \frac{c}{2}\right) \quad (5)$$

In three-point bending, the central deflection *w* of a sandwich beam is the sum of flexural deflection of the face sheets and shear deflection of the core.

$$w = T_1 + T_2 = -\frac{PL^3}{48D} - \frac{PL}{4AG_c} \quad (6)$$

where $A = bd^2/c$, G_c is the honeycomb core's shear modulus, and T_1 and T_2 are flexural and shear deflections at mid-span, respectively.

3.4 Global Buckling of Sandwich Column

When studying sandwich systems, it is generally thought that the core only supports shear and that skins carry tensile and compressive loads under flexure [107]. The contributions of core and skin to flexural and shear stiffness were considered in the sandwich beams examined in this analysis.

Two modes of elastic buckling are possible: Euler buckling mode with sandwich column bending and a core shear mode. The shear deformation of core was taken into

account in a more precise approach [108], [109]. Figure 23 shows the schematic model of buckling setup to find out plane displacement on sandwich beam.

For case of a strut with built-in ends (which are constrained against rotation), the Euler buckling load *PE* is:

$$PE = \frac{4\pi^2 (EI)_{eq}}{l^2} \tag{7}$$

The equivalent flexural stiffness EI_{eq} of the sandwich beams was calculated by Eq. (8).

$$EI_{eq} = \frac{bt^3}{6} E_f + \frac{btd^2}{2} E_f + \frac{bc^3}{12} E_c \tag{8}$$

where E_f and E_c are the Young's moduli of face sheet and core materials, respectively, b is the width of sandwich column, t is the thickness of face sheet, and c is the thickness of core. $d \equiv t + c$ is the distance between the mid-planes of face sheets.

The core shear buckling load *Ps* was set by the shear stiffness of core.

$$Ps = (AG)eq \tag{9}$$

where the corresponding shear rigidity of core $(AG)eq$ is:

$$(AG)eq \approx bcGc \tag{10}$$

where $PS \approx AG_{eq}$, A = $(h + H)2/h$, $G_c = E_c/(1 + 2vc)$, G_c is the shear modulus of the core and bc the cross-sectional area of the core.

However, at transformation values of strut slenderness ratio, these buckling modes interacted to produce a combined collapse load (P_{cr}) where:

$$Pcr = PE + Ps \tag{11}$$

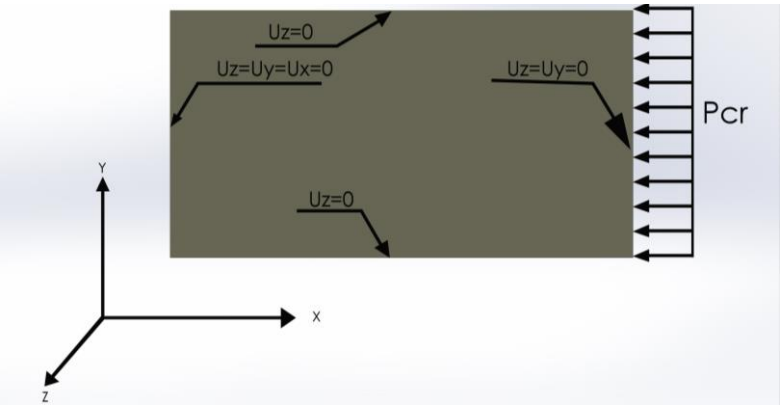

Figure 23: Schematic model of buckling setup

3.5 Heat Transfer Equations

Local heat flux for one-dimensional steady-state heat transfer across a sandwich, according to the Fourier heat transfer law, could be written as:

$$q = -k\Delta T = -k\frac{dT}{dx} \tag{12}$$

where q is local heat flux density (W/m^2), K is material thermal conductivity ($W/m*k$), $\Delta T = \frac{dT}{dx}$ is temperature gradient (K/m).

3.6 Thermal Resistance

Thermal resistance is a thermal property and a measurement of how well a material resists a heat flow.

$$Q_{wall} = -kA\frac{T_2 - T_1}{L} = -\frac{T_2 - T_1}{R_{thcond}} \tag{13}$$

$$Rskin = \frac{t}{K_s A} \tag{14}$$

$$Rcore = \frac{t}{K_c A} \tag{15}$$

$$R_{thcond} = 2(Rskin) + R\ core \tag{16}$$

where ΔT is the amount of heat transited through sandwich beam (T_2 - T_1), R_{thcond} represents thermal conductive resistance, L is length, t is thickness, A is area, K_s is the thermal conductivity of skin and K_c is the thermal conductivity of core. Hence, in this

analysis, temperature was applied on the bottom and top face sheets of the sandwich beam. Figure 24 depicts the schematic model of conductive heat distribution on sandwich beam and showed that high heat was transferred from the top skin, distributed through core and down to bottom skin.

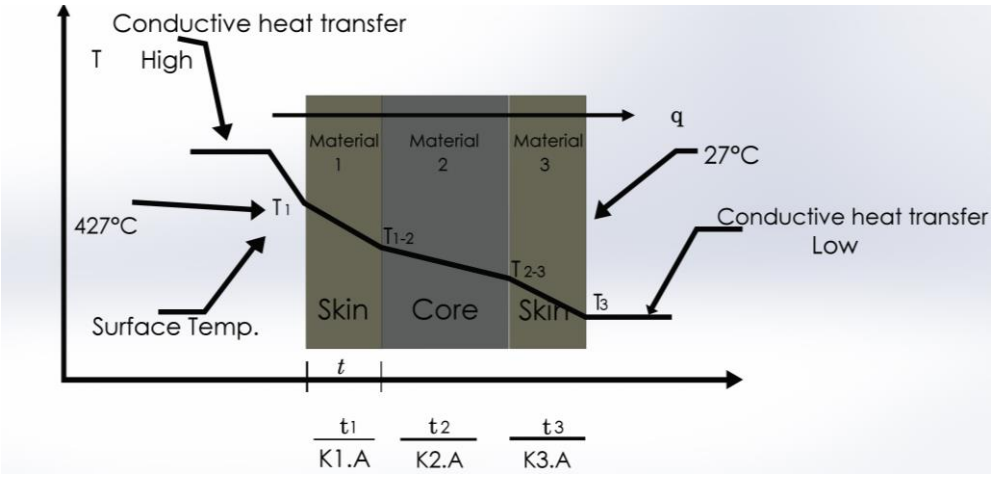

Figure 24: Schematic model of conductive heat distribution on sandwich beam

Chapter 4

RESULTS AND OBSERVATION

4.1 Overview of Study Results

This study aims to investigate the static loading effect on Sandwich beam, its flexural stresses were clearly analyzed and harmonic analysis of the two core shapes was investigated, the amplitude of the response, phase angle and corresponding stresses was detailed. Epoxy carbon UD (230GPa) was used as face skin, aluminum, honeycomb and SAN foam materials used as core. In addition to that, the aluminum alloy was later used as face skin while maintaining honeycomb as the core for validation. The ANSYS finite element method (FEM) simulation results were validated analytically and it is in accordance with the stiffness of the sandwich beams equation. The natural frequency of honeycomb core and mode shapes were illustrated. In order to gain more insight into certain systems' deformation mechanisms, ANSYS is used as the finite element simulation and comparisons between both honeycomb cores materials deformation, stress resistance and mode shapes. Lastly, improved flexural stiffness, resonance resistance and optimization check between the normal hexagonal honeycomb core and proposed shape core are confirmed. In general, sandwich beam heat transfer and thermal strain at corresponding temperature were investigated and compared with added silica aerogel material.

4.2 Deformation and Stresses

The sandwich beam was aligned in 3-point bending test setup, subjected to uniformly distributed load, and point load. Moreover, when a sandwich beam is loaded, internal forces develop within it to maintain equilibrium, in this case the internal forces have 3 components, compression, tension and shear force. Hence, the sandwich beam sagged and became shorter, therefore the internal forces in the top became compressive, as a result, the bottom of the sandwich beam structure got longer and the normal forces in the bottom became tensile. The deformation and the stresses were observed as illustrated in Figure 25. Figure 25(a) shows that the sandwich beam is in compression on the top skin and tension on the bottom skin due to the applied load, the deflection occurs throughout the length of the sandwich beam, starting from the boundary conditions. The stresses keep increasing to the middle of the Sandwich beam where the maximum bending stress and deformation occurred in the mid as shown in Figure 25(b). It is observed that the maximum deflection occurred in the middle of the sandwich beam. Hence, Figure 25(c) shows the rate of deformation of the sandwich beam along its length, starting gradually from both supports and reaching its maximum at the mid. Figure 26 shows a stress plot along the top surface of the hexagonal honeycomb sandwich beam. Figure 26(a) shows the geometry path of the hexagonal sandwich beam created along the top surface. It was investigated that the maximum stress equally occurred at the center of the honeycomb sandwich beam, the hollow nature of the hexagonal made the unstable nature of the line graph to be in a zig-zag manner as depicted in Figure 26(b), it is as a result of errors, moreover the force is either tension or compression along the line. Lastly, Figure 27 depicts the stress plot along the top surface of the proposed honeycomb core model. Similarly, Figure 27(a) shows the geometry path of the proposed sandwich created along the neutral axis while

Figure 27(b) depicts the stresses along the neutral axis. The simulation results plot is shown in Figure 28. Where, the hexagonal honeycomb was assigned 3 different materials and simulated in 3-point bending test, the same number of forces was applied and the stresses recorded for each amount of load, that was repeated for the 3 materials, honeycomb, aluminum alloy and SAN foam. In Figure 29 same simulation setup was carried out but the hexagonal shaped core was replaced with the proposed core model, all results were evaluated and plotted. It was observed that there was significant stress resistance in the proposed model and it is also important to note that aluminum alloy became more elastic than the honeycomb material used in the hexagonal shaped core. To investigate the rate of deformation on sandwich structure for hexagonal shaped core, the materials were assigned and total deformation was recorded and plotted as shown in Figure 30, and same was done for the proposed model in Figure 31. It was observed that the proposed model has reasonable resistance to deformation irrespective of the material used. Finally, Figure 32 shows the effect of core thickness to equivalent von –misses stress and shear stress, it was noted that when the core thickness is increased, both stresses decrease. The findings determined by means of the ANSYS workbench have been compared to the results calculated from the spreadsheet. The analysis of results reveals that the results of the FEM method and the analytical approach have less than 1% difference.

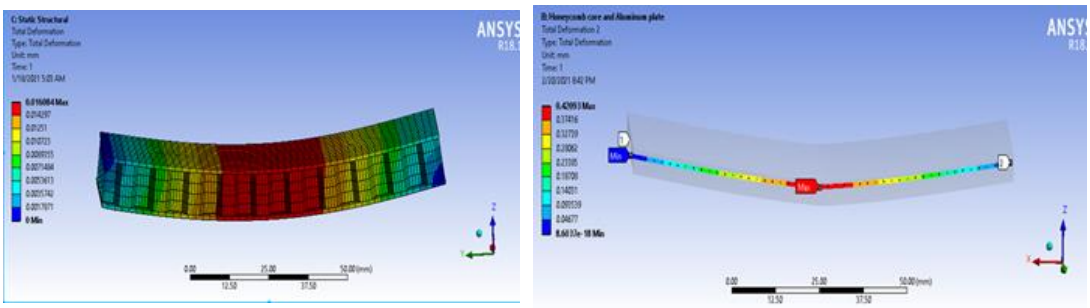

(a) (b)

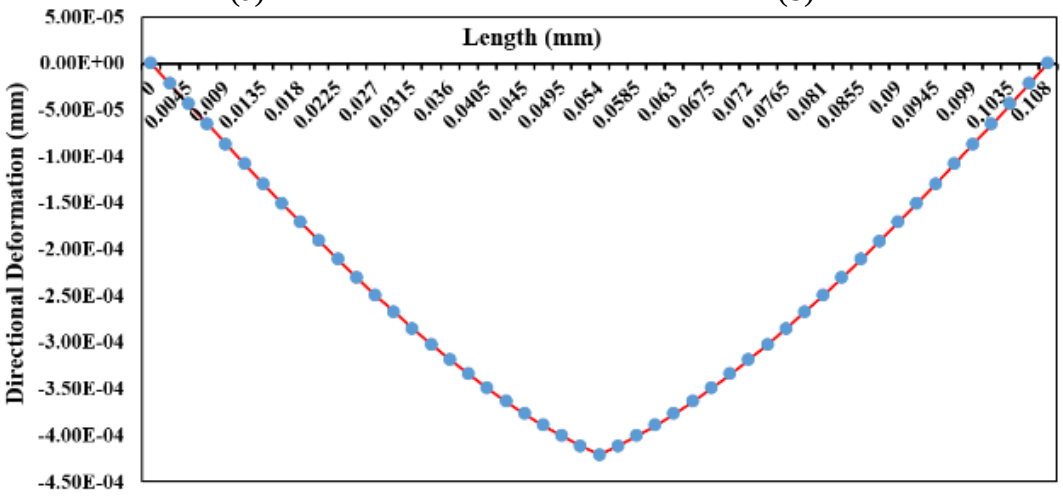

(c)

Figure 25: Deflection along the surface of sandwich structure under 3-point bending loading (a) total deformation of the sandwich beam; (b) maximum deflection at the middle of the sandwich beam; (c) directional deformation along the length of the sandwich beam

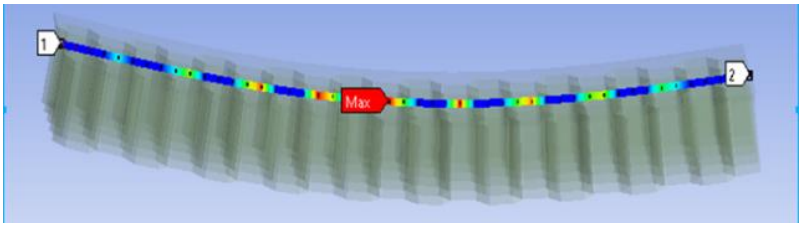

(a)

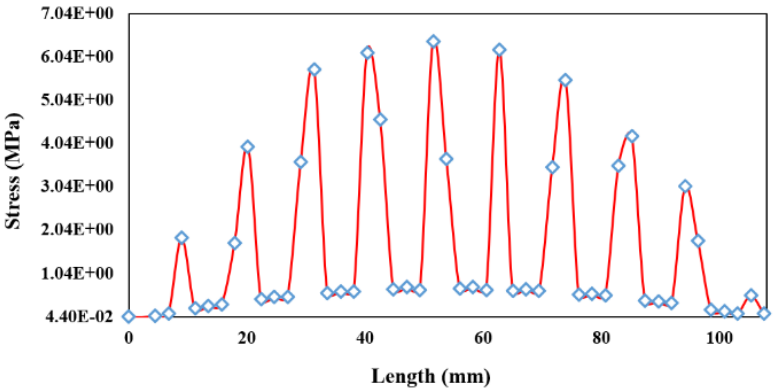

(b)

Figure 26: Stress plot along the top surface of the hexagonal honeycomb structure (a) the geometry path on the top surface of the hexagonal honeycomb structure; (b) stress plot along the length of the hexagonal honeycomb structure

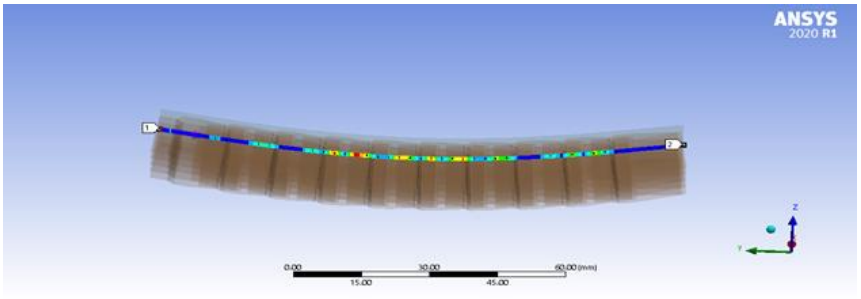

(a)

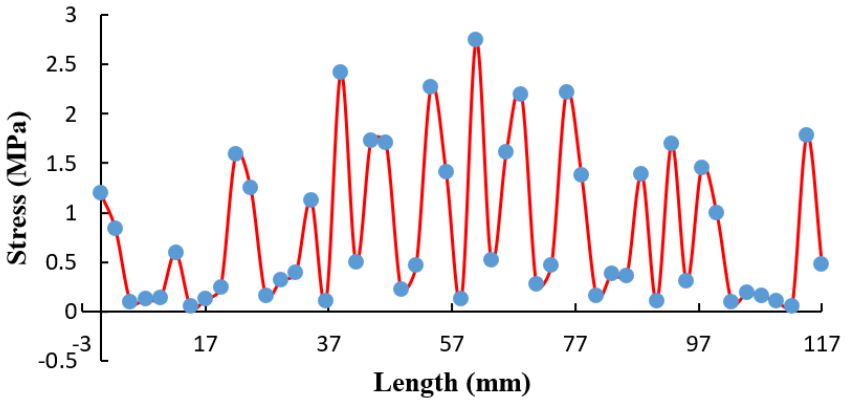

Figure 27: Stress plot along the top surface of the proposed honeycomb structure (a) The geometry path on the top surface of the proposed honeycomb structure; (b) Stress plot along the length of the proposed honeycomb structure

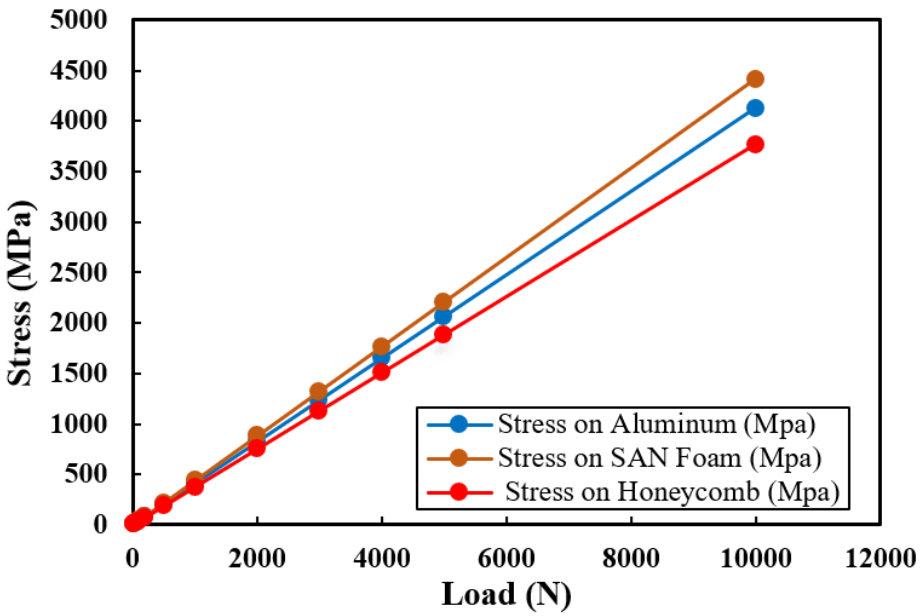

Figure 28: Stresses comparison of hexagonal core materials to Loading

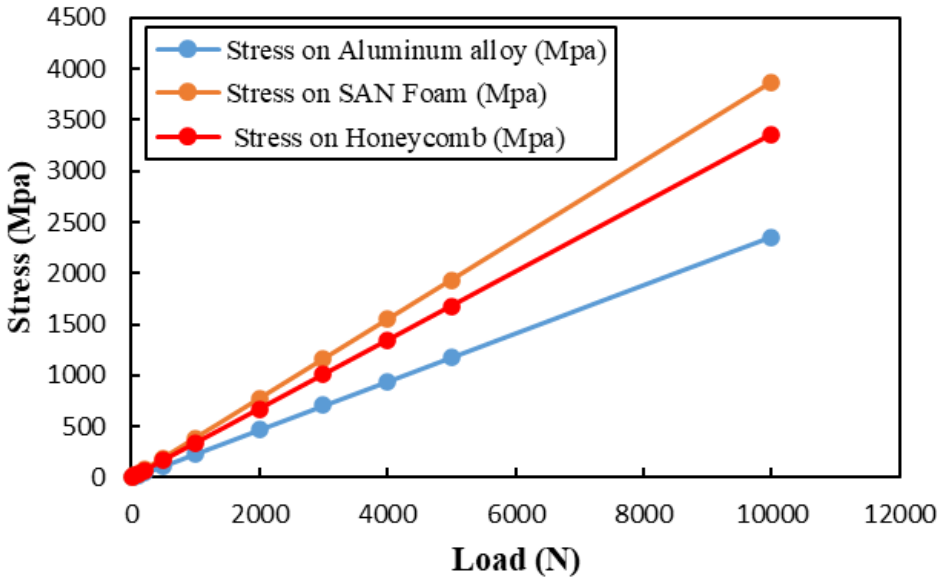

Figure 29: Comparison of proposed core materials to loading

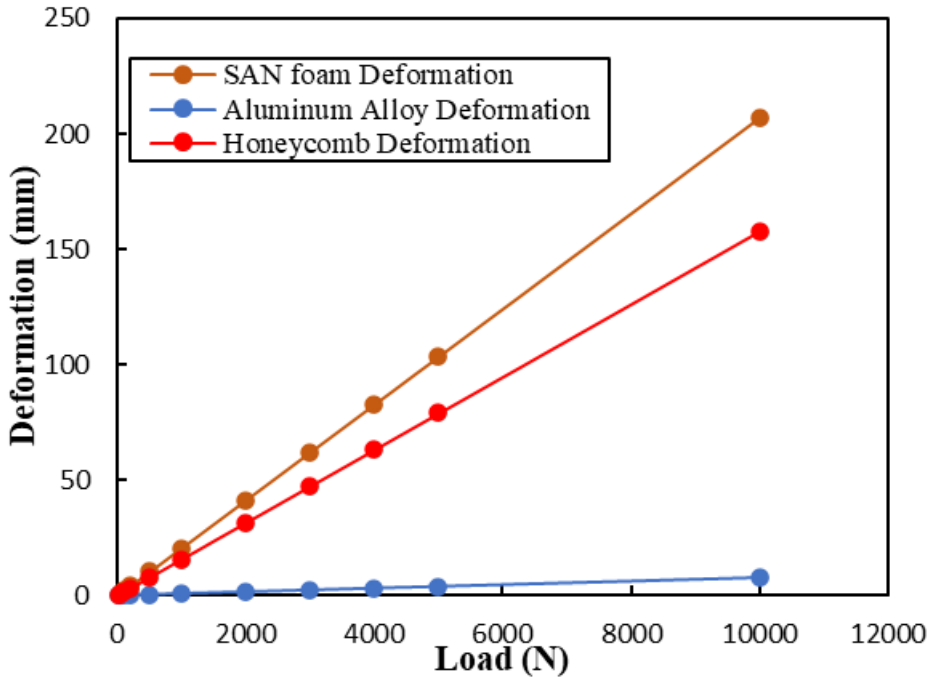

Figure 30: Comparison of sandwich core deformation of hexagonal honeycomb core

Table 8 shows FEM and analytical results of the rate of change in length of the sandwich beam when load of 100 N is applied. The estimated stress of sandwich beam can be obtained from the Eq. (17), combining the stress on the skin and the core. Table 9 depicts the comparison of stresses and validation analysis of sandwich beam structure under 3-point bending test in analytical and FEM.

$$\sigma_s = \frac{M(h/2)}{(EI)_{eq}} E_s \, , \sigma_c = \frac{M(c/2)}{(EI)_{eq}} E_c \tag{17}$$

where h, c, $(EI)_{eq}$, E_c and E_s are sandwich height, core height, flexural stiffness, core young's modulus and skin young's modulus, respectively.

Table 8: Analytical and FEM results at force of 100 N compared

Method	**Strain**
FEM	0.00053102
Analytical	0.00053434

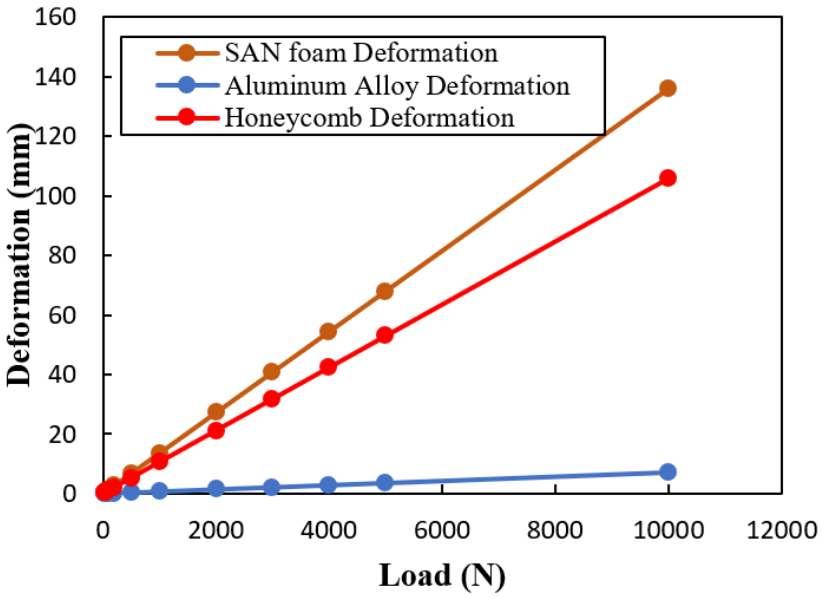

Figure 31: Comparison of sandwich core deformation of proposed geometry core

Similarly, in order to investigate the proposed core model, the same parameter effect of applied load is maintained as used in hexagonal cores simulations. Hence, the behavior was similar with a hexagonal shaped model with improved stress resistance about 10.9%, 12.3%, 42.8% for honeycomb, SAN foam and aluminum alloy respectively. In this case of the proposed shaped geometry simulation, aluminum became more elastic than honeycomb and foam materials compared to the hexagonal shaped core model. Response of sandwich cores deformation in respect to the applied load. It is observed that aluminum core resists deformation more, it has very high compressive strength compared to foam honeycomb cores. Similar to the work done by Aslan et al. [110]. He found that the structure made of carbon fiber and aluminum honeycomb has the highest edgewise compression strength, but poor bending strength, and the structure made of polyurethane foam and carbon fiber has the greatest flat-wise compression strength and bending strength. Moreover, the deformation response of the proposed honeycomb model `is similar to the hexagonal honeycomb shaped core but deformation resistance improved by 32.9%, 12.9%, 34.4% for honeycomb,

aluminum alloy and SAN foam core materials respectively. Stress comparison of sandwich cores materials, aluminum, SAN foam and honeycomb of the same parameter effect of applied load on the hexagonal shaped core. The stress is more on the Foam core and lesser in honeycomb, irrespective of its lowest young's modulus and density. Hence, honeycomb is more elastic than aluminum and foam. Figure 32 shows Effect of core thickness to shear stress and equivalent von –misses stress. Accordingly, as the core thickness increases both stresses decrease, this is in agreement with Potluri et al. [111] work.

Table 9:Equivalent stress comparison of analytical and FEM

Force [N]	**Equivalent Stress Analytical [MPa]**	**Equivalent Stress FEM [MPa]**
10	3.77	3.79
20	7.54	7.59
30	11.31	11.38
40	15.08	15.18
50	18.85	18.97
60	22.62	22.76
70	26.39	26.56
80	30.16	30.35
90	33.93	34.14
100	37.70	37.94

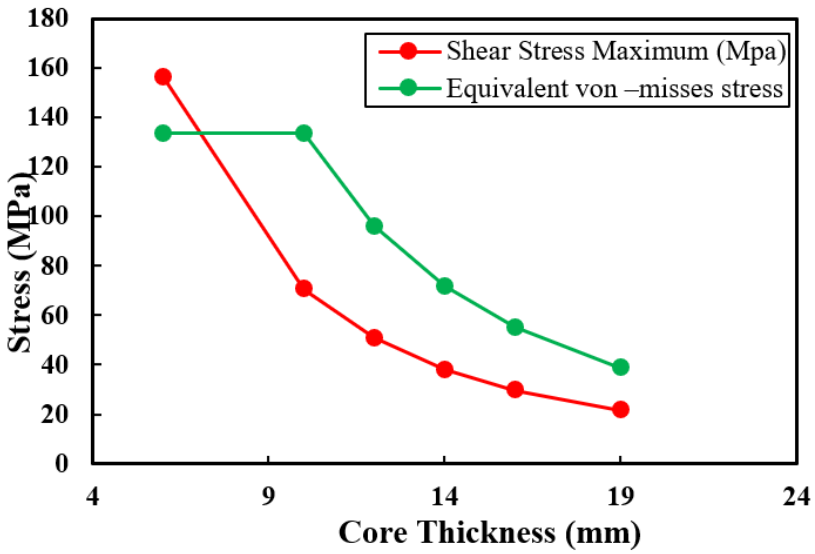

Figure 32: Core thickness vs. stress

4.3 Proposed Honeycomb Core Inclined Edge Model

Hexagonal honeycomb was modified in order to change its geometry to improve its strength and stiffness. Figure 11 is designed from the traditional hexagonal honeycomb structure and modified, with no addition in cell number, both having the same thickness and material. Hence, simulation was carried out in an ANSYS workbench with the same face sheet thickness and material properties, what changed was the core. It was discovered that the new shape has 79.9% deformation resistance, as a result, it is stiffer than a normal hexagonal structure. In general, for stiffer components honeycomb core inclined edge model should be used. Figure 33 illustrates the strain resistance comparison between the hexagonal core sandwich and the proposed core model of the sandwich beam. Hence, in order to investigate the extension of hexagonal shaped core model and proposed shaped core model in ANSYS Workbench mechanical, the sandwich beam was set up and assigned boundary condition in order to mimic the simply supported beam, force ranging from 10 N to100 N was applied as a distributed load on the top surface of the sandwich structure and the corresponding strain recorded and plotted. The simulation was carried out with the same materials, parameters and loading, what changed was the shape of the core. It was observed that when the proposed core shape was used there was a significant reduction in the sandwich beam strain of the proposed shape core model.

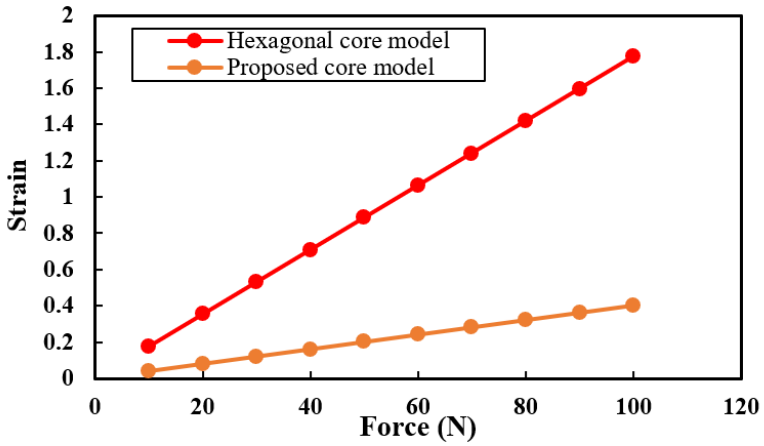

Figure 33: Comparison between the hexagonal honeycomb and proposed sandwich beam

4.4 Analysis and Comparison

Table 10 compares the results of the finite element analysis (FEA) and experimental data approaches done by Boudjemai [112] employed for the modal analysis of the hexagonal honeycomb sandwich beam under clamped-free boundary conditions. For comparison, the first three frequencies have been chosen and results recorded, hence good agreement between the results were obtained. Furthermore, the proposed core sandwich structure was used with the same dimensions and materials as the experimental data provided by Boudjemai in ANSYS and the results were compared as depicted in Table 11. Moreover, the first and third mode of the sandwich are in bending mode, the proposed core model shows great improvement in frequencies that will cause deformation on the sandwich beam, having 12.8% and 30.7% increase for the first and third mode respectively.

Table 10: Results comparison

Frequency	**Finite element analysis**	**Proposed model**	**Experimental** [112]
1	133.45	151.75	134.5
2	309.69	308.21	311
3	818.51	929.69	711

4.5 Modal Analysis and Natural Frequencies

In order to determine vibration characteristics, that is natural frequency and mode shapes of honeycomb sandwich structure. Natural frequency of sandwich beam system are the frequencies at which it vibrates with increasing amplitude. Hence, the phenomenon is referred to as resonance. Figure 34 shows the mode shapes of first 6 natural frequencies on sandwich beam structure with core thickness of 10 mm and face thickness of 1mm. Figure 35 depicts the mode shapes of natural frequency of honeycomb core and lastly Figure 36 shows the first 6 modes shapes of natural frequency of proposed core. In addition, it has significant effect on the shear stresses. This is due to the differences in mass and stiffness which is caused by variation in core and skin thickness of the honeycomb sandwich beam. Additionally this is in accordance with Upreti et al. [113] and Potluri et al. [111] work. Table 11 shows natural frequencies of honeycomb sandwich beam structure, hexagonal honeycomb core and proposed core model.

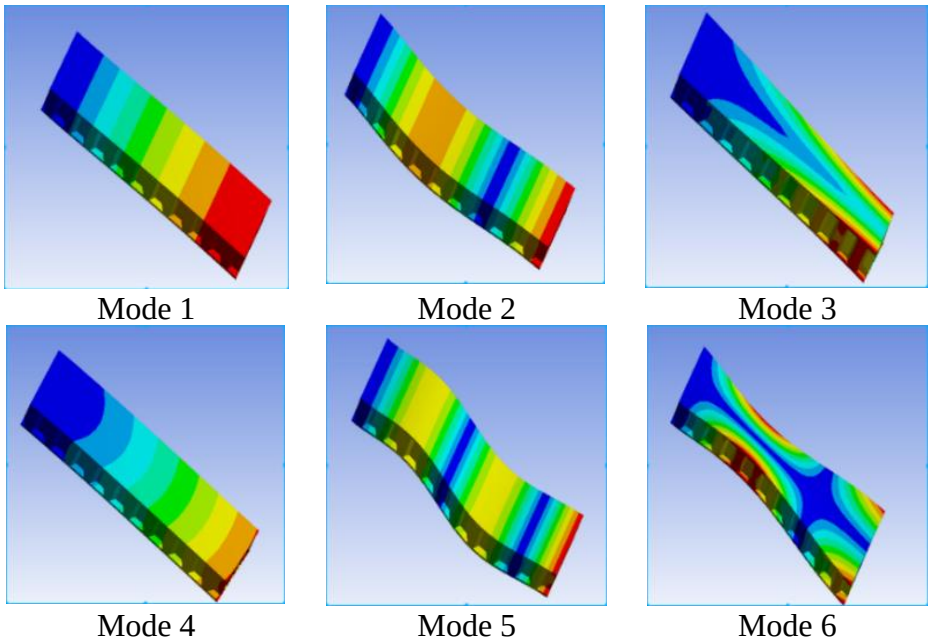

Figure 34: First 6 mode shapes contours of the sandwich structure

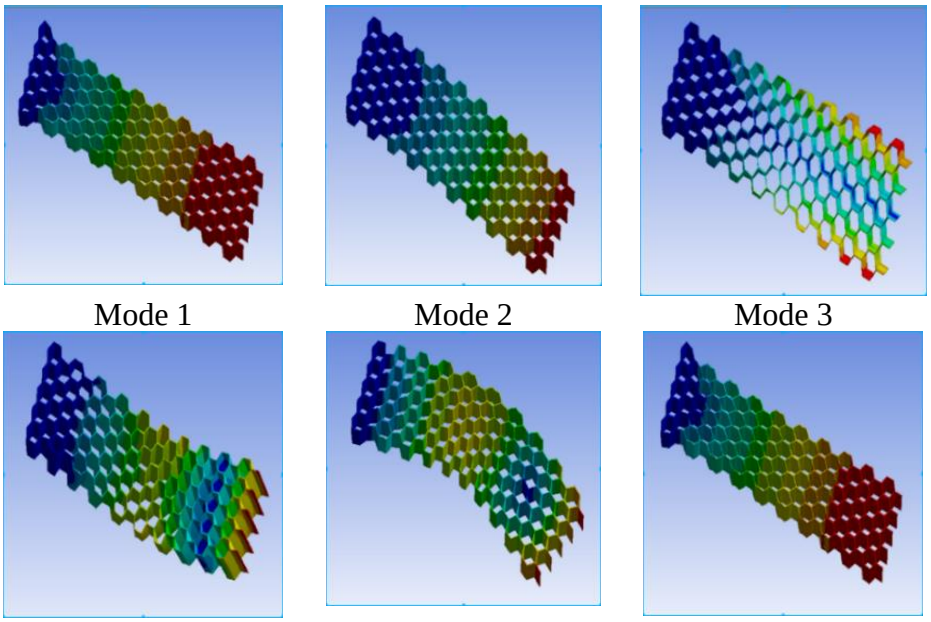

Mode 1 Mode 2 Mode 3

Mode 4 Mode 5 Mode 6

Figure 35: First 6 mode shapes contours of honeycomb core

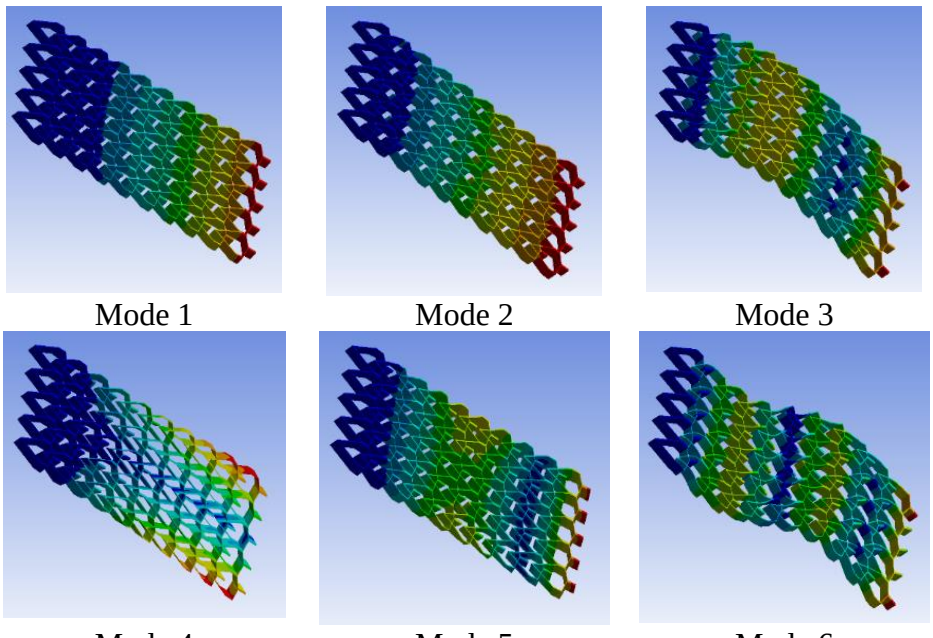

Mode 1 Mode 2 Mode 3

Mode 4 Mode 5 Mode 6

Figure 36: First 6 mode shapes contours of proposed model

Table 11: Natural frequency

Mode	Natural Frequency of Sandwich beam (Hz)	Total Deformation of Sandwich beam (mm)	Natural Frequency of Honeycomb core model (Hz)	Total deformation of Honeycomb core model (mm)	Natural Frequency of Proposed core model (Hz)	Total Deformation of Proposed core model (mm)
1	196.53	480.87	113.11	759.24	322.50	342.64
2	622.53	525.62	227.38	704.13	359.64	283.82
3	661.36	795.44	618.00	911.05	1242.30	317.00
4	990.69	680.32	702.54	819.35	1317.30	425.78
5	1148.40	583.92	1078.10	685.84	1868.20	382.03
6	1547.20	794.27	1327.30	507.74	2489.20	366.01

4.6 Honeycomb Solid and Equivalent Model Natural Frequency

ACP in ANSYS Workbench was used to develop two types of Honeycomb sandwich beam that gives approximately same the results, a similar study was performed by Rahman et al. [114]. Figure 37 shows the equivalent model designed from ACP where all the necessary material parameter are assigned. The solid model shown in Figure 38 is also designed from the ACP and added solid layer, Hence, using both is effective when considering the kind of boundary condition needed to apply. In addition, Table 12 depicts the difference in their nodes and elements and Table 13 shows the closeness of the equivalent model and Solid model of sandwich beam mode results. The difference in their results is negligible, the equivalent model takes lesser time due to lower numbers of nodes and elements. A similar test was carried for the loading and deformation, it was found out that equivalent models run faster than the solid model. In addition, the solid model was added Resin epoxy which made it stiffer than the equivalent model. In general, both models can be used for any analysis. This is in accord with Rahman et al. [114] study on the efficiency of continuum, discrete and

equivalent models. The complex cellular geometry is converted into a set of effective continuum properties that can be employed in most sandwich calculations using these models.

Table 12: Nodes and elements of both models

Model	Nodes	Elements
Solid	11928	10153
Equivalent Shell	994	923

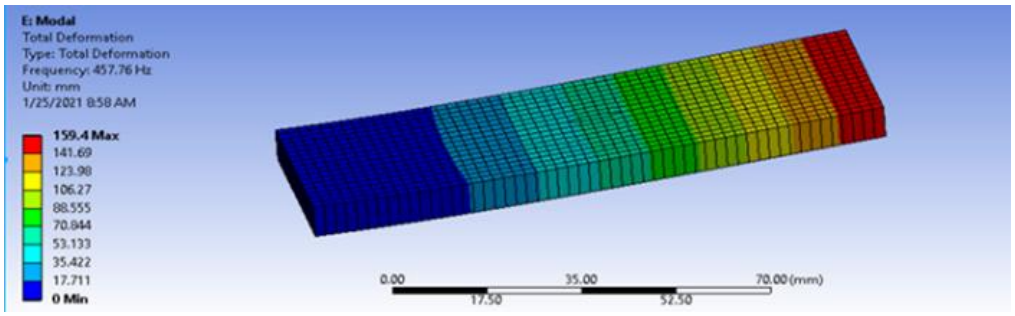

Figure 37: Honeycomb sandwich beam structure equivalent model

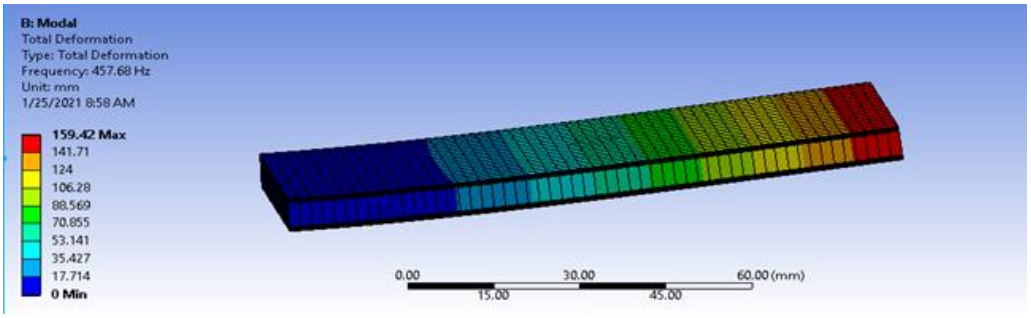

Figure 38: Honeycomb sandwich beam structure solid model

Table 13: Natural frequency comparison of equivalent model and Solid model

Mode	Equivalent Frequency (Hz)	Solid Frequency (Hz)
1	457.76	457.68
2	2166.1	2181.5
3	2362	2364.3
4	2817	2819.2
5	6858.5	6915.8
6	7692.5	7710.8

4.6.1 Dynamic Analysis and Harmonic Analysis

In order to effectively understand the significance of hexagonal honeycomb and the proposed honeycomb model designs, harmonic analysis is carried out. Additionally, the linear dynamics of forced frequency response analysis in the frequency domain of both models is observed.

4.6.2 Hexagonal Honeycomb Model

In order to investigate the behavior of honeycomb structure under steady-state sinusoidal (harmonic) loading at a given frequency. Moreover, the time-history response of the honeycomb will be ignored in this analysis. Therefore, considering the honeycomb structure dynamic behavior in the frequency domain instead of the time domain. The 2 modes are spread over a frequency sweep from 0 to 900 Hz, modes with higher frequencies were ignored for this analysis. Hence, a single harmonic force of 100 N was applied in Z-axis orientation as shown in Figure 39 in order to obtain a reasonable resolution, the solution interval was made 50 and damping control ratio of 2%. Figure 40 depicts the frequency response plot of the honeycomb core, the peak frequencies were observed but for more accurate results in capturing the peak, a cluster was added for more resolution. In general, the frequency at which peak deformation occurs is 108 Hz, where the honeycomb core experiences the most deformation. However, with respect to this, contour results were created and evaluated as shown in

Figure 41, while Figure 42 depicts the phase response plot. lastly, considering the equivalent stresses, the model is set to the peak frequency of 108 Hz and the corresponding sweeping angle is the same as the directional deformation plot and was evaluated as shown in Figure 43. In conclusion, based on the design criteria more material or functionally graded material should be added in the region of a yellowish part to bring the stresses within a preferred reach, in order to enable the honeycomb structure to overcome fatigue, and other harmful effects of forced vibration. The input and output of harmonic analysis are both sinusoidal acting at the same excitation frequency.

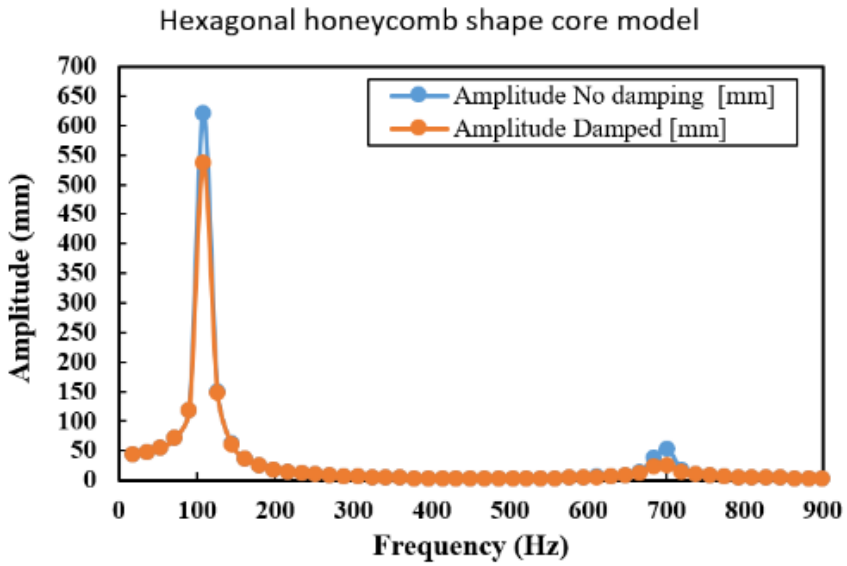

Figure 39: Frequency (Hz) vs amplitude (mm) plot (maximum displacement in amplitude is dictated)

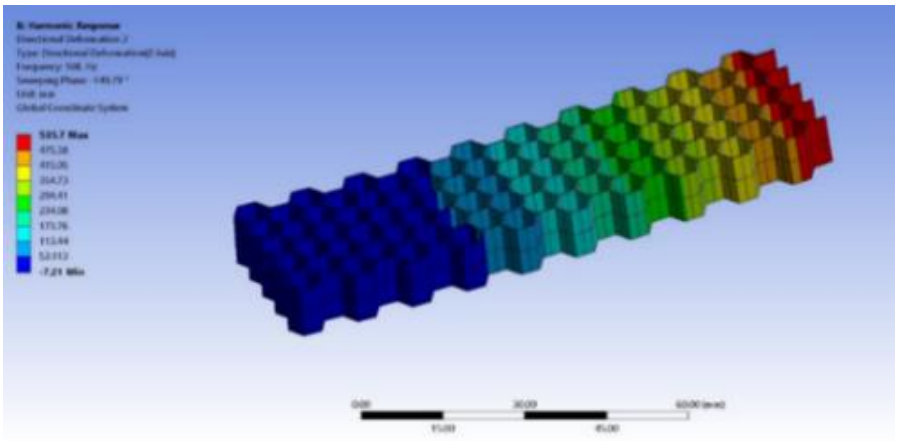

Figure 40: 108 Hz the maximum deformation occurred at the corresponding peak response and sweep angle 0f 149.79

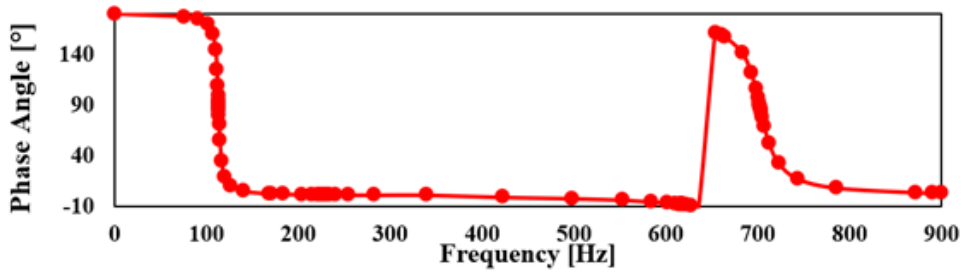

Figure 41: Phase response plot

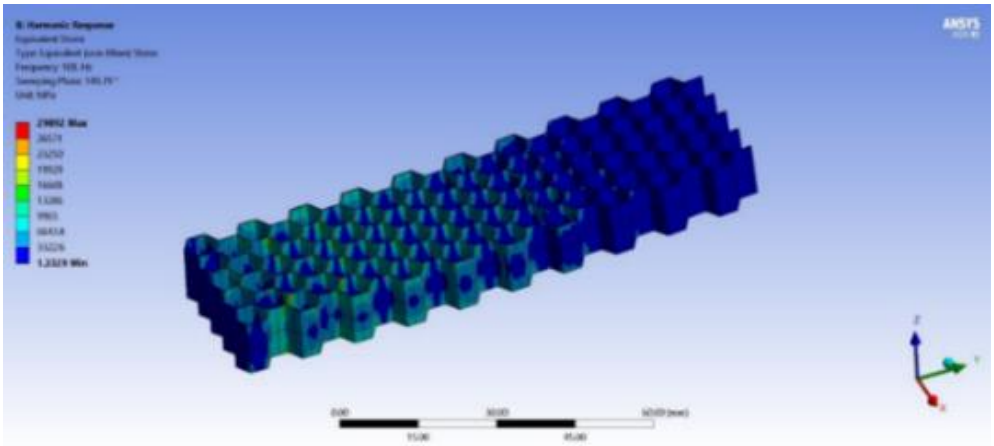

Figure 42: Equivalent stresses acting on the honeycomb core at the peak response.

4.6.3 Proposed Shape Honeycomb Core Model

Similarly, the same steps were carried out as in hexagonal harmonic analysis for the proposed model. Figure 43 shows the frequency response plot, Figure 44 depicts the contour plot on the core, Figure 45 illustrates the phase response plot of the proposed

model and lastly, Figure 46 shows the point of maximum bending. Hence, a damping ratio for the core is defined as 2%, under the harmonic system, a force of 100 N was applied in the Z direction and having the frequency sweep from 0 to 900 Hz. Moreover, the frequency at which peak deformation occurs is 324 Hz, the local results were recorded in Table 14. However, as a result of that, the peak displacement occurs at the first natural frequency from the modal analysis of 324 Hz while maximum spatial resolution is used. It is observed that the maximum value reported from the frequency response plot Figure 43 corresponds with the peak value on the contour plot as shown in Figure 44.

Table 14: Analysis and results

Model	**Maximum Frequency (Hz)**	**Phase angle (°)**	**Directional deformation (mm)**	**Equivalent stress (MPa)**	**Frequency Sweep (Hz)**	**Harmonic Force (N)**
Hexagonal core	108	149.79	535.70	29892.00	0 - 900	100
Proposed core	324	93.614	69.76	21297.00	0 - 900	100

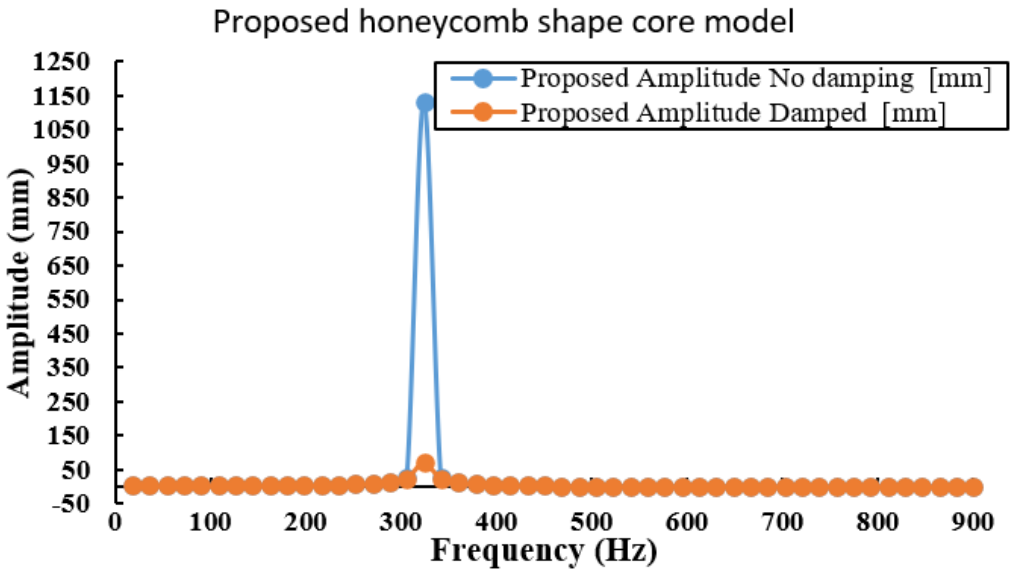

Figure 43: Harmonic analysis of proposed honeycomb shape core frequency response plot (maximum displacement in amplitude is dictated)

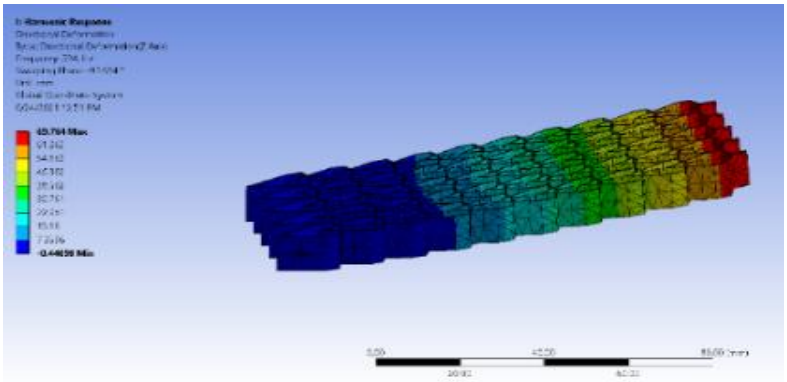

Figure 44: Harmonic analysis of proposed honeycomb shape core directional deformation on the core at 324 hz (contour plot)

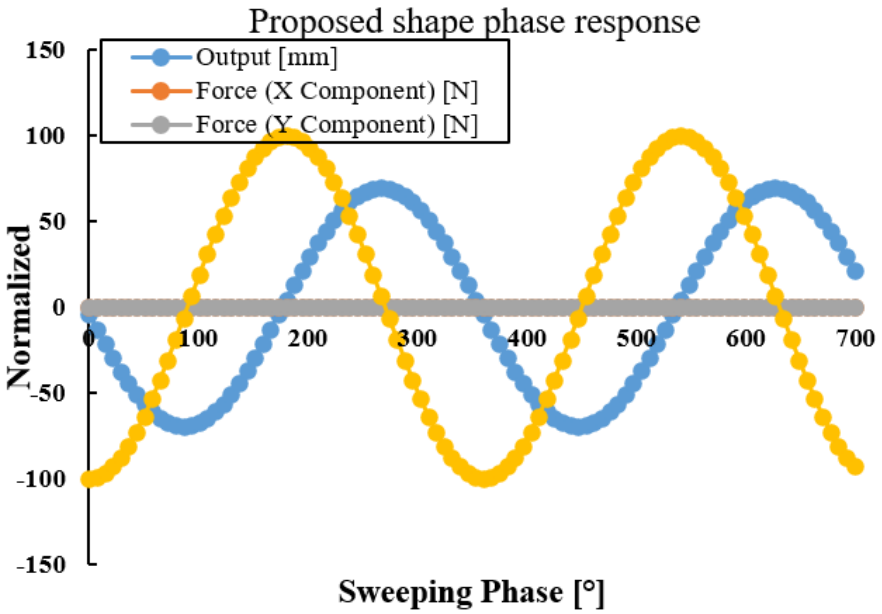

Figure 45 Harmonic analysis of proposed honeycomb shape core 93.61° reflect a phase shift between the sinusoidal input loads and corresponding response due to 2% damping assumed in the proposed honeycomb model

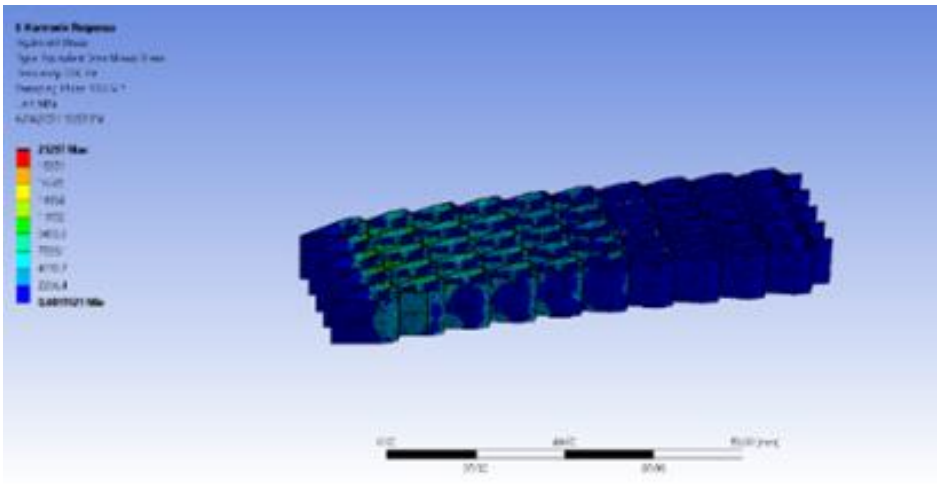

Figure 46: Harmonic analysis of proposed honeycomb shape core, equivalent stresses acting on the proposed honeycomb core at the peak response (point of maximum bending

4.6.4 Buckling Analysis

In order to determine the failure mode in which relatively large deflections occurred on sandwich beam, buckling analysis was carried out to investigate what load and temperature level caused buckling and elastic instability on sandwich structures. Moreover, sandwich deformation nature was investigated by determining the

temperature that buckled the sandwich, according to the material properties used for sandwich beam. Furthermore, simulation was carried out on two sandwich beams, one with carbon fiber strut in the core and the other without carbon fiber strut. Figure 47 and Figure 48 depicts the buckling nature of the sandwich beam without carbon fiber strut. Furthermore, the same procedure was applied to observe the buckling nature of the sandwich with imbedded strut as shown in Figure 49, Figure 50 and Figure 51. In this case, temperature was not added in static structural analyzer and the results showed improvement in buckling load for the sandwich with carbon fiber circular strut, as shown in Table 15.

Table 15: Buckling load

Sandwich type	**Buckling Load (N)**
Sandwich with circular strut imbedded in core	34413
Sandwich without circular strut	31017

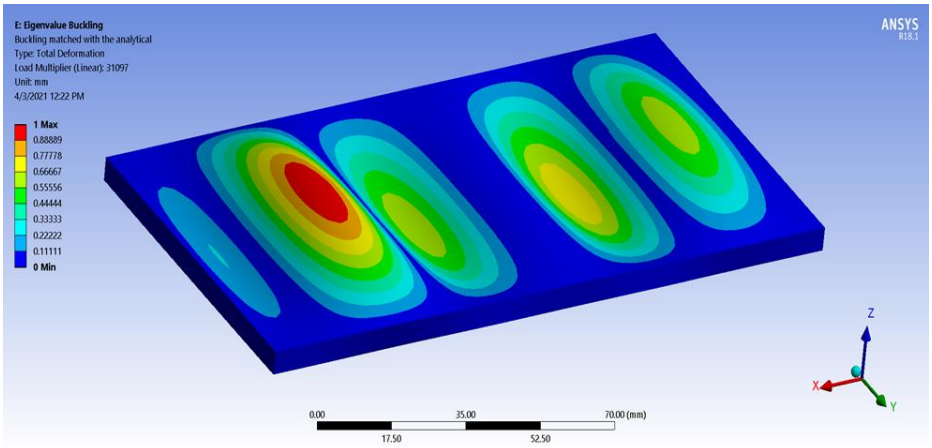

Figure 47: Buckling of sandwich under axial compression (isometric view)

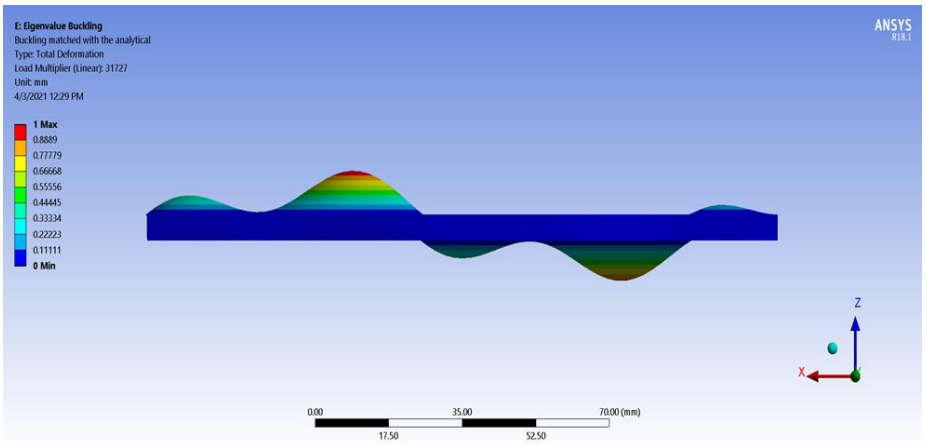

Figure 48: Buckling of sandwich under axial compression (side view)

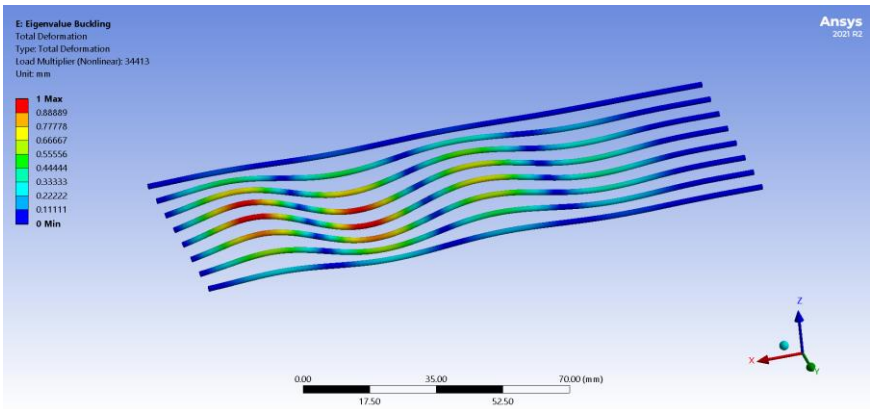

Figure 49: Cylindrical carbon fiber imbedded in the core (diameter of 1.5 mm)

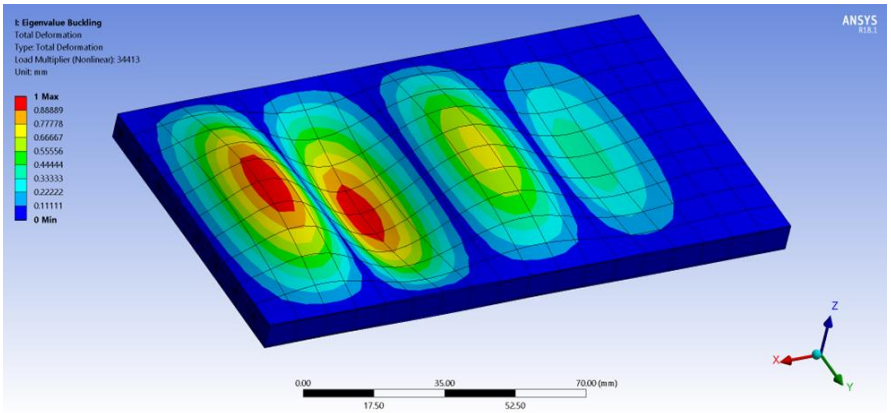

Figure 50: Buckling of sandwich under axial compression (isometric view)

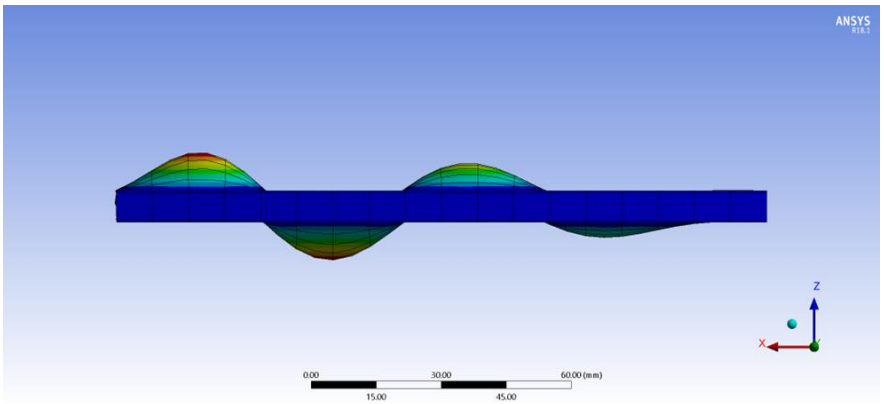

Figure 51: Buckling of sandwich under axial compression (side view**)**

4.6.5 Buckling Analysis with Thermal Expansion

Nonlinear buckling performed in a static structural analysis in Ansys Workbench mechanical. The temperature was raised and sandwich buckling were observed. To begin with, the analysis settings in structural run was set and large deflection turned on. In addition, the boundary assigned, the x movement on both sides were constraint to confine the sandwich beam during thermal expansion in order to observe the compressive stresses in x-direction. Furthermore, the sandwich vertex were prevented from moving in z-direction and lastly the left and right sandwich beam edges were restricted from moving vertically. In general, the sandwich beam cannot thermally expand in the x-direction, only in y-direction and z-direction due to the constraint, it is not free to translate and rotate globally.

4.6.6 Load

Environment temperature of 70°F was assigned to the sandwich beam in static structural analysis, and thermal condition of the sandwich beam is 100 °F. Hence, in this analysis there is 30 °F temperature increase that will cause thermal expansion and we get the thermal stress. As a results of that, solution transferred to eigenvalue buckling module in order to observe the temperature that will cause state of stresses, the first mode shapes is what was expected as both sides of the sandwich beam was

quizzed and not allowed to move globally, it buckles up in the middle. Hence, as there is 30 °F difference which is the only load on the sandwich beam and that is multiplied by load multiplier of the first mode in the eigenvalue buckling module and summed with the environmental temperature assigned early which is 70°F, therefore the temperature that will cause buckling in the sandwich beam was recorded, same analysis was repeated for sandwich with aerogel layers, and the buckling temperature was equally noted. Figure 52 shows the mode 1 of sandwich beam without silica aerogel. Moreover, the first mode is what is considered the most. Figure 53 shows the aerogel position in the sandwich beam, Figure 54 and Figure 55 shows the first and second mode shapes of sandwich beam with silica aerogel material respectively. Table 16 shows the temperature that will cause buckling on both sandwich beam, with and without aerogel layers. There is 6% increase in temperature that can buckle the sandwich beam when silica aerogel is used.

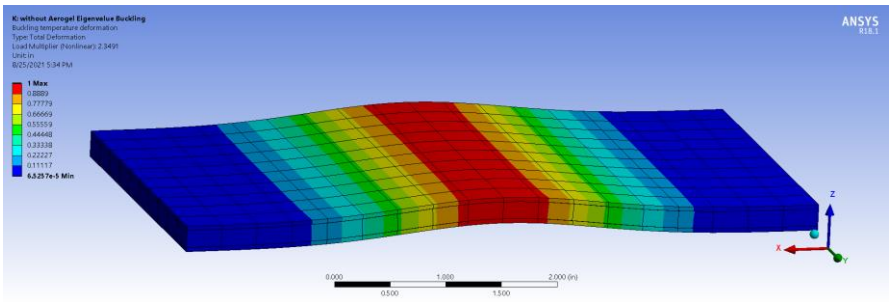

Figure 52: Mode shapes of sandwich beam without silica aerogel (mode 1)

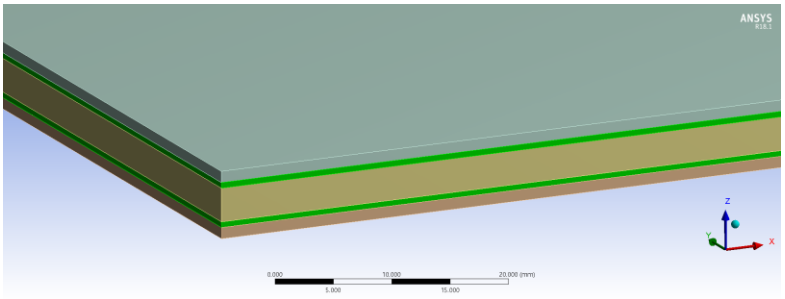

Figure 53: Sandwich beam with silica aerogel addition

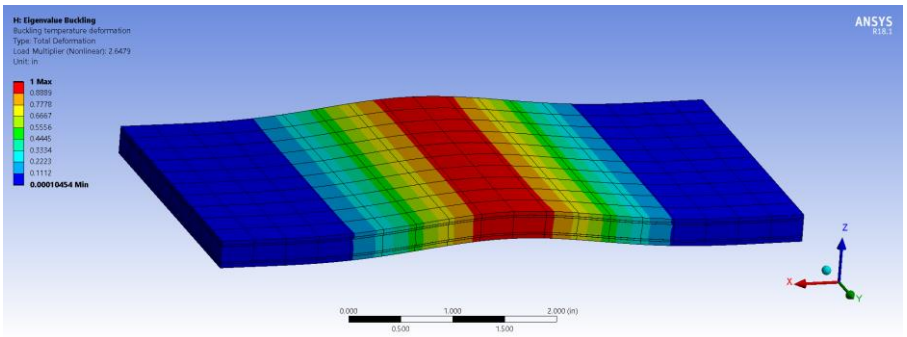

Figure 54: Mode 1 shapes of sandwich beam with silica aerogel

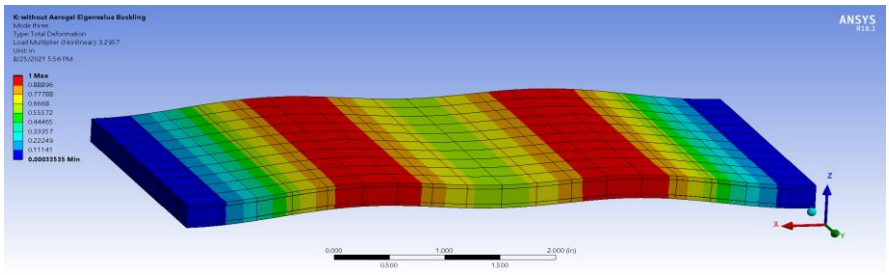

Figure 55: Mode 2 shapes of sandwich beam with silica aerogel

Table 16: Buckling temperature

Sandwich type	Buckling Temperature (°F)
Sandwich with silica aerogel	149.44
Sandwich without silica aerogel	140.47

4.6.7 Conduction Thermal Analysis of Sandwich Beam and Stresses

In order to investigate heat transfer, Sandwich structure was made of more than one material, thermal loads and effective factors of the sandwich were observed. Moreover, a change in temperature produced thermal strains which could cause sandwich deformation. The analysis was conducted under steady state thermal module in ANSYS and the solution was imported into static structural module for the observation of thermal strain and mechanical stress. Temperature of 427 °C was applied to top skin and 22 °C to bottom skin. It was assumed that the sandwich beam was used as cover structure which emitted high temperature. The effects of temperature increase from bottom face sheet to top face sheet (T = 22°C to 427 °C) for the sandwich of carbon

fiber-polyimide face skin and carbon foam core are shown in Figure 56. At high temperatures, thermal stress was increased from minimum to maximum causing expansion on the top face, as shown in Figure 57. Hence, there was some deformation in bottom skin (contraction), as shown in Figure 58. Similarly, silica aerogel with the thickness of 0.5 mm was added as shown in Figure 59. The corresponding thermal strain nature of the sandwich beam. As a result of considering the heat conduction of the sandwich, based on review [115], carbon fiber-polyimide and carbon foam materials were used. Figure 60 shows the deformation of aerogel layer on the hot side while Figure 61 depicts the thermal deformation of aerogel material only bonded between top skin and core. In addition, Figure 62 shows thermal strain on the bottom skin of the sandwich beam. It was found that thermal strain was minimal on the sandwich beam due to the addition of silica aerogel layers and the top skin did not deform so much as compared when silica aerogel was not added. In general, it was observed that there was significant decrease in heat flux when silica aerogel was added, as depicted in Figure 63. Sandwich beam was subjected to high temperature ranging from 100 °C to 430 °C and the corresponding heat flux was recorded for sandwich beams with and without aerogel material. The results showed that the sandwich beam with silica aerogel had significant heat transfer resistance, as shown in Figure 64. Similarly, simulation was repeated, in this case thermal deformation was considered and results showed that sandwich beam with aerogel layers had good thermal strain resistance, as depicted in Figure 65. However, thermal deformation was decreased by 17.6% when silica aerogel was added as layer. In this analysis, 0.5 mm aerogel layer improved thermal strain by about 17.6%.

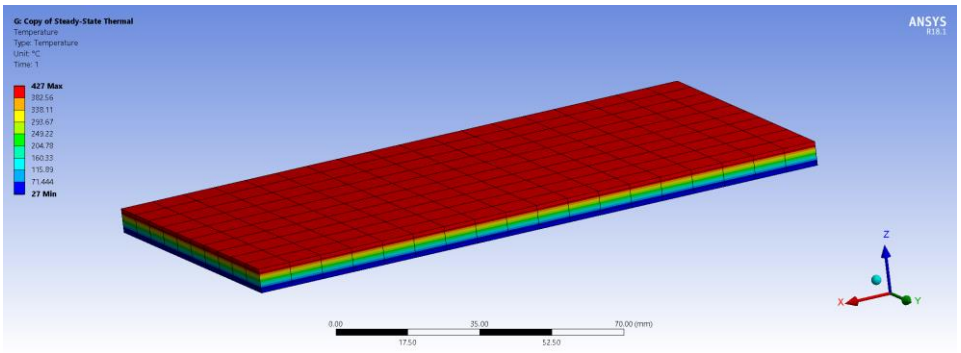

Figure 56: Temperature distribution across the top and bottom skins, temperature increasing from T = 27 °C to 427 °C

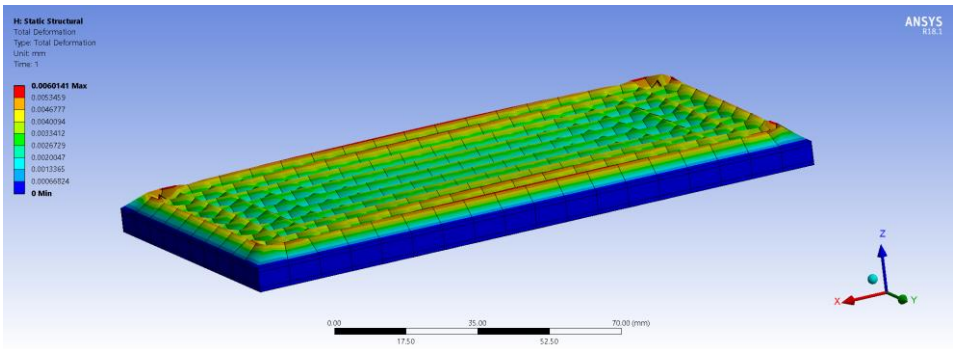

Figure 57: Sandwich structure showing deformation on the top face at 427 °c (carbon foam core used)

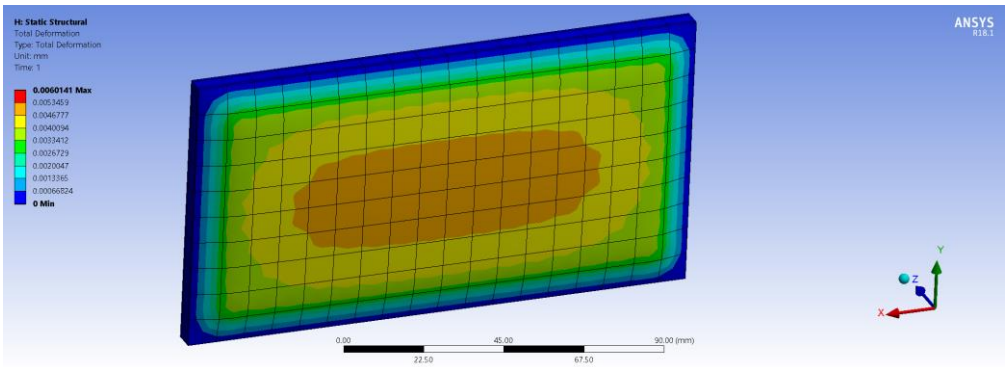

Figure 58: Sandwich structure showing deformation on the bottom face at 427 °c

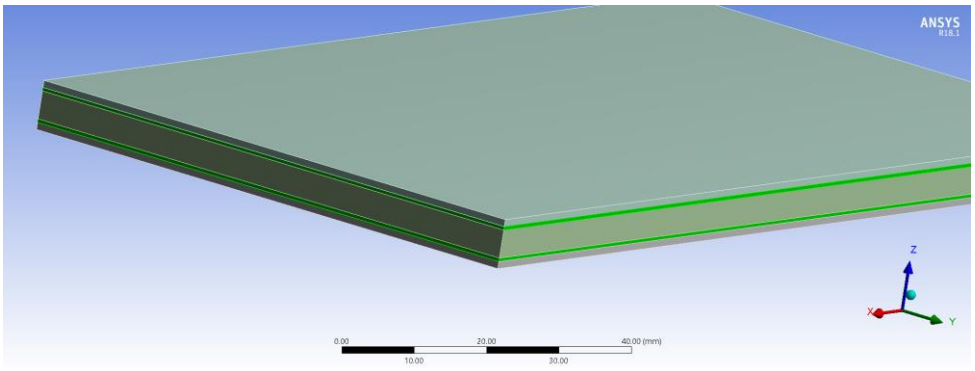

Figure 59: Sandwich structure with silica aerogel layer

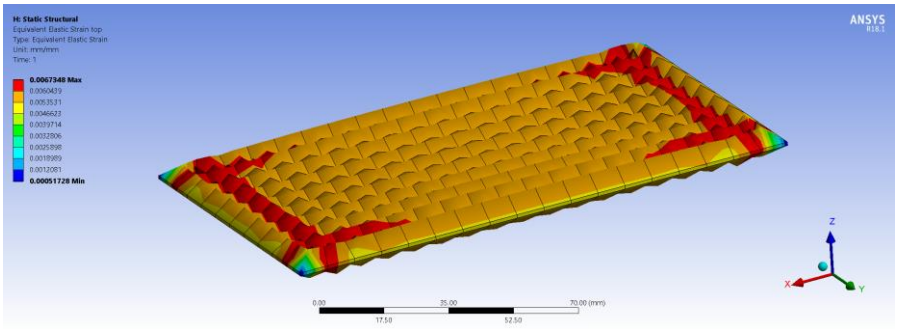

Figure 60: Thermal strain on top skin

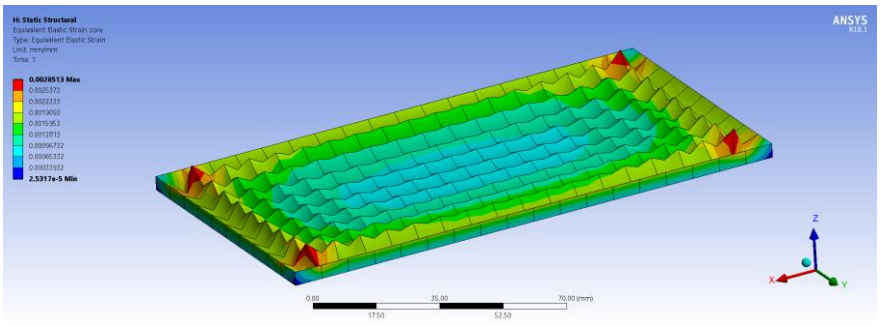

Figure 61: Thermal strain on core

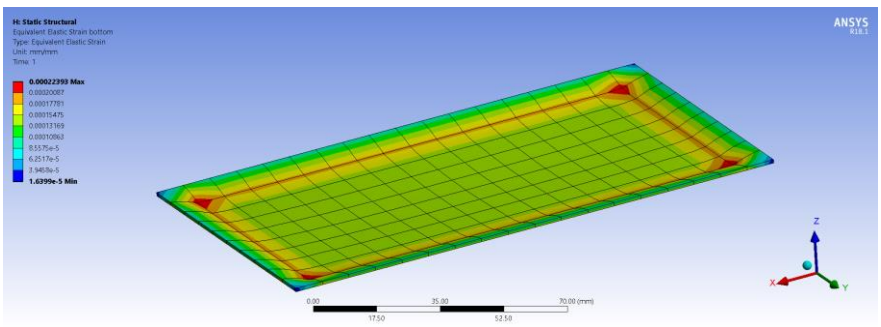

Figure 62: Thermal strain on bottom skin (scale 0.5x auto)

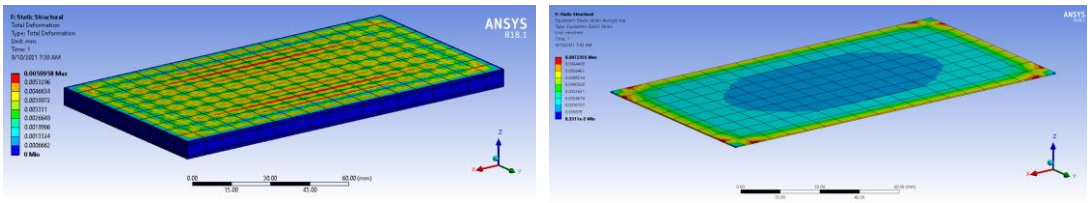

(a) (b)

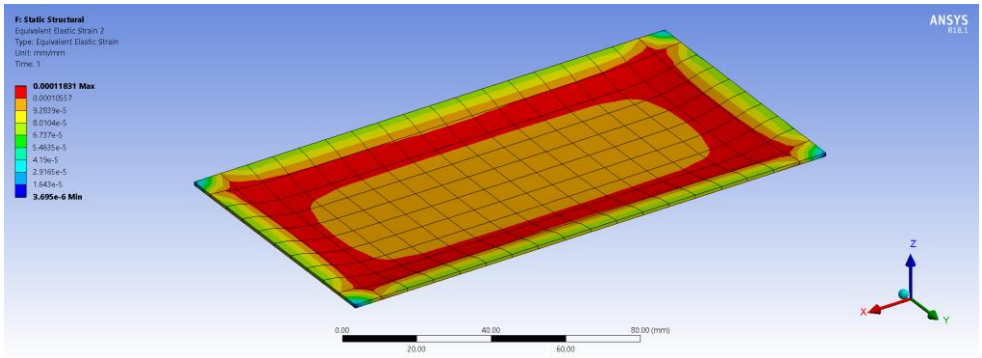

(c)

Figure 63: Sandwich with aerogel layer. (a) Sandwich structure showing deformation on the top face at 427 °C (carbon foam core and aerogel layer used); (b) Thermal strain on top aerogel layer; (c) thermal strain on bottom skin

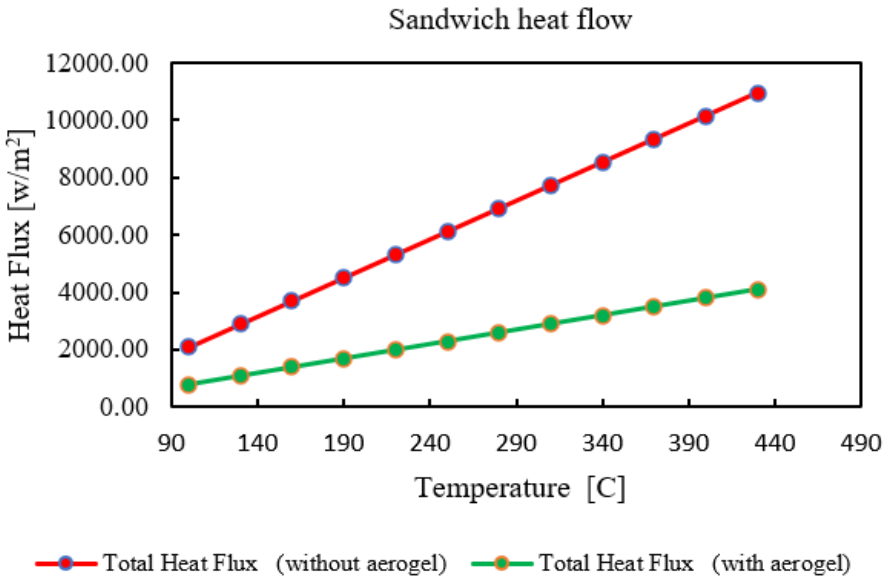

Figure 64: Change in temperature vs. heat flux of sandwich

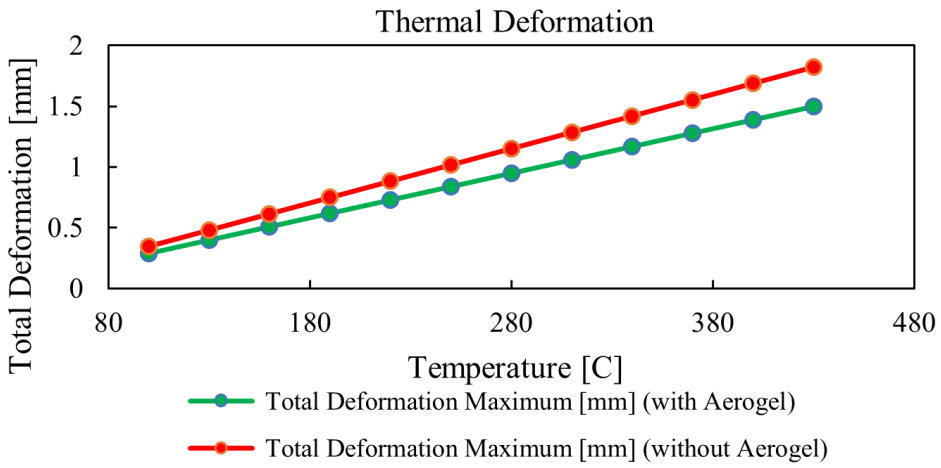

Figure 65: Change in temperature vs. thermal deformation of sandwich beam

4.6.8 Analysis and Comparison for Sandwich Heat Flux

The experimental approaches developed by Goswami [116] were simulated and modified. Goswami used aramid sheet for skin and aramid hexagonal honeycomb core, filled with silica aerogel. The setup was separated into two parts: heating system (part A) where heater installed on the top face sheet of the sandwich with thermocouple arrangements and only the thermocouple was installed on the bottom face sheet (part B). Temperature increase stopped at 350 ºC because the manufacturer specified that the flash point of silica aerogel as to be 395 ºC.

Figure 66 shows heat flux on honeycomb sandwich panel in three cases;

1) Honeycomb filled with silica aerogel.

2) Honeycomb with silica aerogel as auxiliary face sheet.

3) Honeycomb without silica aerogel.

The results showed that honeycomb with silica aerogel as auxiliary face sheet had lower heat flux, thereby providing a good heat insulation in honeycomb sandwich beam.

In ANSYS workbench, thermal analysis experiment was simulated and the results were validated. Moreover, honeycomb filled with silica aerogel as shown in Figure 67 has higher temperature difference (The heat will take longer to transfer from one side to the other) than the one without silica aerogel as depicted in Figure 68 Furthermore, the methods used by Goswami in the experiment was by no means the most effective approach towards providing heat insulation in honeycomb sandwich as there was much heat flow in honeycomb cell walls, as shown in Figure 69. In general, silica aerogel was used as auxiliary face sheet before the honeycomb hexagonal core as depicted in Figure 70. Therefore, heat flow was minimal and evenly distributed through honeycomb core, as shown in Figure 71.

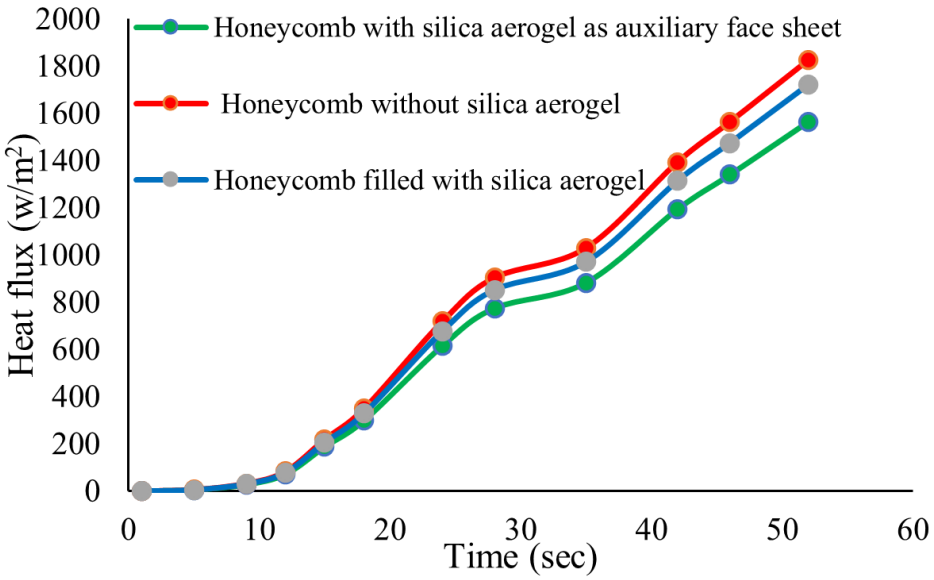

Figure 66: Time vs. heat flux of sandwich panel

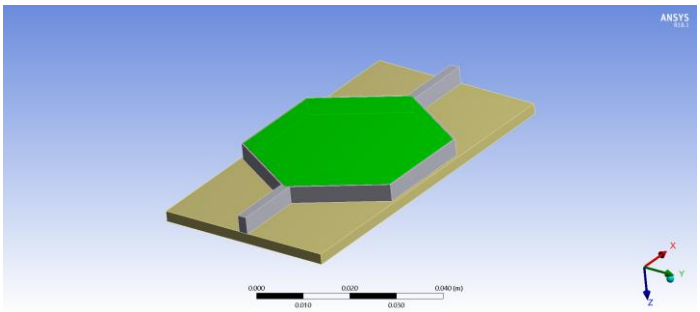

Figure 67: Honeycomb filled with silica aerogel

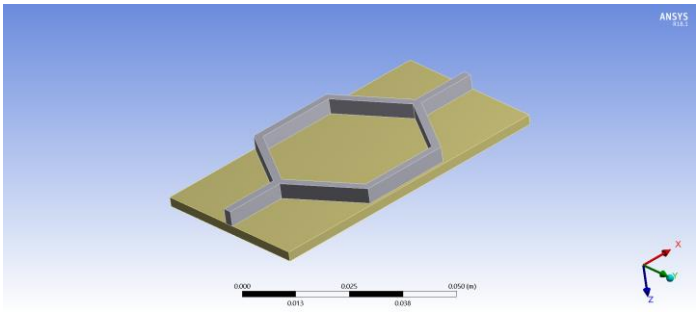

Figure 68: Honeycomb without silica aerogel

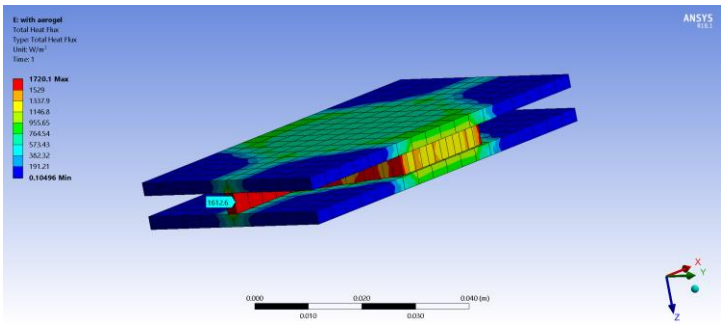

Figure 69: Heat flow in honeycomb cell walls on honeycomb filled with silica aerogel

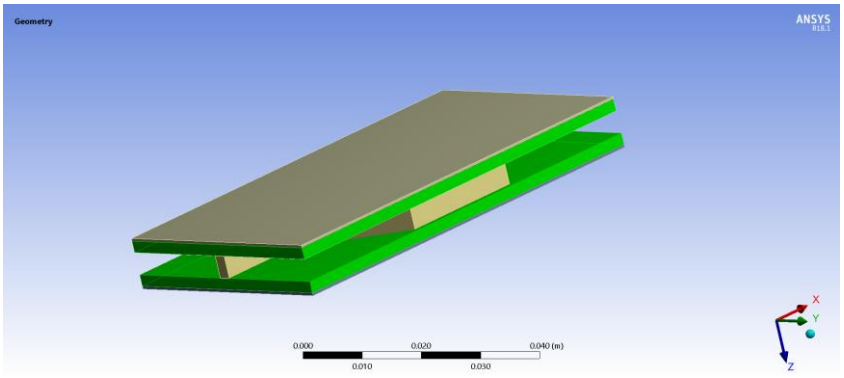

Figure 70: Silica aerogel as auxiliary face sheet

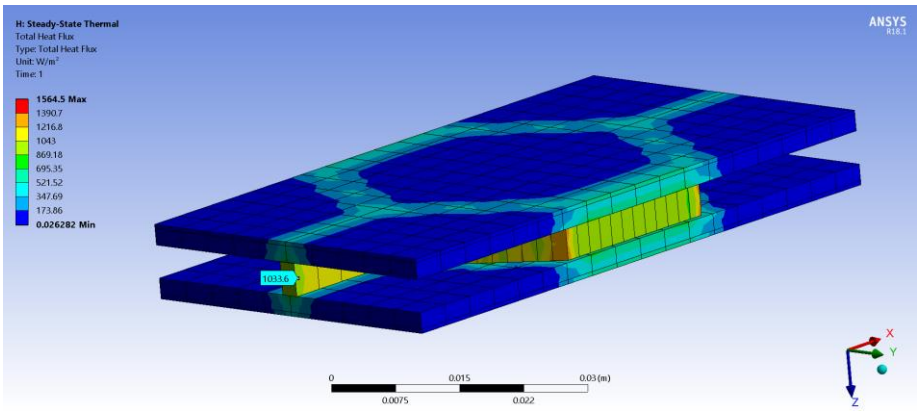

Figure 71: Reduced heat flow on core cell walls (silica aerogel as auxiliary face sheet)

Chapter 5

CONCLUSIONS

A comprehensive analysis and simulation were carried out and the results were depicted and plotted, and essential observation was noted. The stresses reviewed from the peak frequencies of both cores were analyzed, it was observed that the proposed core model has fewer stresses and deformation at a much higher frequency than the traditional hexagonal honeycomb core, it is clear that the distribution of mass and stiffness in the proposed core model is better than the hexagonal shaped core as compared with the experimental results. The core thickness and thickness of the face sheet have a significant effect on shear stress, deformation and equivalent maximum stress. Hence, increasing the thickness of the face sheets is the least efficient way to accomplish a rigid sandwich beam (not including the cost involved, especially when producing in large quantities), it would increase the weight exponentially. Nevertheless, it was well observed that the type of core material affects it elastic behavior and strength of the sandwich beam. The thickness of the skin is directly proportional to mass and inversely proportional to the sandwich beam structure's elastic strain. As a result of the simulation compared, the proposed shape core has 79.9% extension resistance more than the hexagonal shape core. Moreover, the equivalent sandwich beam model is the fastest to solve computationally, while the discrete sandwich beam model takes a longer time.

Thermal stresses and buckling temperature were improved by the addition of silica aerogel material. Steady state condition of sandwich beam was investigated in commercial software ANSYS and temperature induced stress and the nature of thermal expansion-induced deformation were noted. Hence, parameters affecting thermal strain and heat flow were mechanical properties and the most significant one was thermal conductivity, as we considered the heat conduction of sandwich beam (heat flux). In addition, experimental approach was simulated and modified. Filling hexagonal honeycomb cells with silica aerogel was not the most effective way of heat reduction in sandwich but it could be used as auxiliary face sheet. Moreover, carbon foam with lower thermal conductivity was further improved by the addition of silica aerogel layer which was the lightest and hence, had the mass of 1.22 g and extreme heat flow resistance. As a result of flexural strength, sandwich was imbedded with cylindrical bar carbon fiber strut in the core, thereby improving stiffness and buckling load. Addition of carbon fiber strut was effective in maintaining flexural strength while keeping the core thickness minimal.

In general, we can conclude that sandwich beam structure with carbon fiber skin layers is stiffer than metal skins, lighter and weigh lesser. In addition, it was investigated that ply angle orientation has a significant effect on strength of the sandwich beam, same with the number of layers, but increasing the layers will equally increase the overall weight, instead the core thickness should be increased. In the situation of modal analysis, it was found that an increase in skin layers and core thickness increases the natural frequency, this is due to higher and lower stiffness in the modes. Therefore, the natural frequency was found to increase as core height increased. This is in line with a typical plate structure's vibration behavior. In the future, material selection for ductile failure and effect on loading in an uncontrolled environment of honeycomb sandwich

beam structure should be clearly evaluated and the proposed shape of the core should have experimented with functionally graded materials for more optimal results.

REFERENCES

[1] V. Pandyaraj, A. Rajadurai, and G. Anand, "Experimental investigation of compression strength in novel sandwich structure," *Mater. Today Proc.*, vol. 5, no. 2, Part 2, pp. 8625–8630, 2018, doi: https://doi.org/10.1016/j.matpr.2017.11.561.

[2] Ş. Sorohan, M. Sandu, A. Sandu, and D. M. Constantinescu, "Finite Element Models Used to Determine the Equivalent In-plane Properties of Honeycombs," *Mater. Today Proc.*, vol. 3, no. 4, pp. 1161–1166, 2016, doi: 10.1016/j.matpr.2016.03.013.

[3] G. Ghongade, K. P. Kalyan, R. V. Vignesh, and M. Govindaraju, "Design, fabrication, and analysis of cost effective steel honeycomb structures," *Mater. Today Proc.*, vol. 46, pp. 4520–4526, 2021.

[4] C. Qiu, Z. Guan, X. Guo, and Z. Li, "Buckling of honeycomb structures under out-of-plane loads," *J. Sandw. Struct. Mater.*, vol. 22, no. 3, pp. 797–821, 2020, doi: 10.1177/1099636218774383.

[5] Z. Zhang, Q. Zhang, D. Zhang, Y. Li, F. Jin, and D. Fang, "Enhanced mechanical performance of brazed sandwich panels with high density square honeycomb-corrugation hybrid cores," *Thin-Walled Struct.*, vol. 151, p. 106757, 2020, doi: https://doi.org/10.1016/j.tws.2020.106757.

[6] A. W. Alshaer and D. J. Harland, "An investigation of the strength and stiffness

of weight-saving sandwich beams with CFRP face sheets and seven 3D printed cores," *Compos. Struct.*, vol. 257, p. 113391, 2021, doi: https://doi.org/10.1016/j.compstruct.2020.113391.

[7] M. F. Ashby and L. J. Gibson, "Cellular solids: structure and properties," *Press Synd. Univ. Cambridge, Cambridge, UK*, pp. 175–231, 1997.

[8] M. Hussain, R. Khan, and N. Abbas, "Experimental and computational studies on honeycomb sandwich structures under static and fatigue bending load," *J. King Saud Univ. - Sci.*, vol. 31, no. 2, pp. 222–229, 2019, doi: 10.1016/j.jksus.2018.05.012.

[9] V. N. Burlayenko and T. Sadowski, "Analysis of structural performance of sandwich plates with foam-filled aluminum hexagonal honeycomb core," *Comput. Mater. Sci.*, vol. 45, no. 3, pp. 658–662, 2009, doi: 10.1016/j.commatsci.2008.08.018.

[10] S. Darzi, H. Karampour, H. Bailleres, B. P. Gilbert, and D. Fernando, "Load bearing sandwich timber walls with plywood faces and bamboo core," *Structures*, vol. 27, no. February, pp. 2437–2450, 2020, doi: 10.1016/j.istruc.2020.08.020.

[11] D. GAY and V. Suong, "HOA a Stephen W. TSAI," *Compos. Mater. Des. Appl.*, 2003.

[12] M. F. Ashby and D. CEBON, "Materials selection in mechanical design," *Le J.*

Phys. IV, vol. 3, no. C7, pp. C7-1, 1993.

[13] L. J. Gibson, "Cellular solids," *Mrs Bull.*, vol. 28, no. 4, pp. 270–274, 2003.

[14] M. A. Douville and P. Le Grognec, "Exact analytical solutions for the local and global buckling of sandwich beam-columns under various loadings," *Int. J. Solids Struct.*, vol. 50, no. 16–17, pp. 2597–2609, 2013, doi: 10.1016/j.ijsolstr.2013.04.013.

[15] F. Zhang, W. Liu, Z. Ling, H. Fang, and D. Jin, "Mechanical performance of GFRP-profiled steel sheeting composite sandwich beams in four-point bending," *Compos. Struct.*, vol. 206, pp. 921–932, 2018, doi: https://doi.org/10.1016/j.compstruct.2018.08.034.

[16] K. M. A. Sohel and J. Y. Richard Liew, "Steel–Concrete–Steel sandwich slabs with lightweight core — Static performance," *Eng. Struct.*, vol. 33, no. 3, pp. 981–992, 2011, doi: https://doi.org/10.1016/j.engstruct.2010.12.019.

[17] G. Reyes, "Static and low velocity impact behavior of composite sandwich panels with an aluminum foam core," *J. Compos. Mater.*, vol. 42, no. 16, pp. 1659–1670, 2008, doi: 10.1177/0021998308092216.

[18] A. G. Mamalis, K. N. Spentzas, D. E. Manolakos, M. B. Ioannidis, and D. P. Papapostolou, "Experimental investigation of the collapse modes and the main crushing characteristics of composite sandwich panels subjected to flexural loading," *Int. J. Crashworthiness*, vol. 13, no. 4, pp. 349–362, Jul. 2008, doi:

10.1080/13588260801933691.

[19] V. Crupi, G. Epasto, and E. Guglielmino, “Collapse modes in aluminium honeycomb sandwich panels under bending and impact loading,” *Int. J. Impact Eng.*, vol. 43, pp. 6–15, 2012, doi: https://doi.org/10.1016/j.ijimpeng.2011.12.002.

[20] J. R. Correia, M. Garrido, J. A. Gonilha, F. A. Branco, and L. G. Reis, “GFRP sandwich panels with PU foam and PP honeycomb cores for civil engineering structural applications: Effects of introducing strengthening ribs,” *Int. J. Struct. Integr.*, 2012.

[21] Y. Qin, R. Kang, J. Sun, Y. Wang, X. Zhu, and Z. Dong, “A fast self-calibration method of line laser sensors for on-machine measurement of honeycomb cores,” *Opt. Lasers Eng.*, vol. 152, no. January, p. 106981, 2022, doi: 10.1016/j.optlaseng.2022.106981.

[22] J. F. Davalos, P. Qiao, X. Frank Xu, J. Robinson, and K. E. Barth, “Modeling and characterization of fiber-reinforced plastic honeycomb sandwich panels for highway bridge applications,” *Compos. Struct.*, vol. 52, no. 3, pp. 441–452, 2001, doi: https://doi.org/10.1016/S0263-8223(01)00034-4.

[23] G. Camata and P. B. Shing, “Static and fatigue load performance of a gfrp honeycomb bridge deck,” *Compos. Part B Eng.*, vol. 41, no. 4, pp. 299–307, 2010, doi: https://doi.org/10.1016/j.compositesb.2010.02.005.

[24] G. Kalaprasad, P. Pradeep, G. Mathew, C. Pavithran, and S. Thomas, “Thermal conductivity and thermal diffusivity analyses of low-density polyethylene composites reinforced with sisal, glass and intimately mixed sisal/glass fibres,” *Compos. Sci. Technol.*, vol. 60, no. 16, pp. 2967–2977, 2000, doi: https://doi.org/10.1016/S0266-3538(00)00162-7.

[25] S. Sahraoui, E. Mariez, and M. Etchessahar, “Mechanical testing of polymeric foams at low frequency,” *Polym. Test.*, vol. 20, no. 1, pp. 93–96, 2000, doi: https://doi.org/10.1016/S0142-9418(00)00006-4.

[26] J. M. Quintana and T. M. Mower, “Thermomechanical behavior of sandwich panels with graphitic-foam cores,” *Mater. Des.*, vol. 135, pp. 411–422, 2017.

[27] N. K. Subedi and N. R. Coyle, “Improving the strength of fully composite steel-concrete-steel beam elements by increased surface roughness—an experimental study,” *Eng. Struct.*, vol. 24, no. 10, pp. 1349–1355, 2002, doi: https://doi.org/10.1016/S0141-0296(02)00070-6.

[28] N. K. Subedi, “Double skin steel/concrete composite beam elements: experimental testing,” *Struct. Eng.*, vol. 81, no. 21, pp. 30–35, 2003.

[29] I. M. Daniel and J. L. Abot, “Fabrication, testing and analysis of composite sandwich beams,” *Compos. Sci. Technol.*, vol. 60, no. 12–13, pp. 2455–2463, 2000, doi: 10.1016/S0266-3538(00)00039-7.

[30] L. Vaikhanski and S. R. Nutt, “Fiber-reinforced composite foam from

expandable PVC microspheres," *Compos. Part A Appl. Sci. Manuf.*, vol. 34, no. 12, pp. 1245–1253, 2003, doi: 10.1016/S1359-835X(03)00255-0.

[31] B. K. Hadi and F. L. Matthews, "Development of Benson–Mayers theory on the wrinkling of anisotropic sandwich panels," *Compos. Struct.*, vol. 49, no. 4, pp. 425–434, 2000, doi: https://doi.org/10.1016/S0263-8223(00)00077-5.

[32] E. E. Gdoutos, I. M. Daniel, and K.-A. Wang, "Compression facing wrinkling of composite sandwich structures," *Mech. Mater.*, vol. 35, no. 3, pp. 511–522, 2003, doi: https://doi.org/10.1016/S0167-6636(02)00267-3.

[33] W. Jiang and Y. Liu, "Indentation of rigidly supported sandwich beams with core gradation," *Int. J. Mech. Sci.*, vol. 134, pp. 182–188, 2017, doi: https://doi.org/10.1016/j.ijmecsci.2017.10.014.

[34] Z. Li, X. Chen, B. Jiang, and F. Lu, "Local indentation of aluminum foam core sandwich beams at elevated temperatures," *Compos. Struct.*, vol. 145, pp. 142–148, 2016, doi: https://doi.org/10.1016/j.compstruct.2016.02.083.

[35] G. X. Ha, D. Marinkovic, and M. W. Zehn, "Parametric investigations of mechanical properties of nap-core sandwich composites," *Compos. Part B Eng.*, vol. 161, no. December 2018, pp. 427–438, 2019, doi: 10.1016/j.compositesb.2018.12.108.

[36] T. M. McCormack, R. Miller, O. Kesler, and L. J. Gibson, "Failure of sandwich beams with metallic foam cores," *Int. J. Solids Struct.*, vol. 38, no. 28, pp. 4901–

4920, 2001, doi: https://doi.org/10.1016/S0020-7683(00)00327-9.

[37] G. X. Ha, M. W. Zehn, D. Marinkovic, and C. Fragassa, “Dealing with Nap-Core Sandwich Composites: How to Predict the Effect of Symmetry,” *Materials (Basel).*, vol. 12, no. 6, p. 874, 2019.

[38] J. W. Fu, A. H. Akbarzadeh, Z. T. Chen, L. F. Qian, and D. Pasini, “Non-Fourier heat conduction in a sandwich panel with a cracked foam core,” *Int. J. Therm. Sci.*, vol. 102, pp. 263–273, 2016, doi: 10.1016/j.ijthermalsci.2015.11.011.

[39] K. Mehar and S. Kumar Panda, “Thermal free vibration behavior of FG-CNT reinforced sandwich curved panel using finite element method,” *Polym. Compos.*, vol. 39, no. 8, pp. 2751–2764, 2018, doi: 10.1002/pc.24266.

[40] S. Sun, Y. Sheng, S. Feng, and T. Jian Lu, “Heat transfer efficiency of hierarchical corrugated sandwich panels,” *Compos. Struct.*, vol. 272, p. 114195, 2021, doi: https://doi.org/10.1016/j.compstruct.2021.114195.

[41] R. Moradi-Dastjerdi and K. Behdinan, “Dynamic performance of piezoelectric energy harvesters with a multifunctional nanocomposite substrate,” *Appl. Energy*, vol. 293, no. April, p. 116947, 2021, doi: 10.1016/j.apenergy.2021.116947.

[42] B. Su, J. Chen, J. Hao, X. Fan, and X. Han, “Thermal insulation performance of GFRP squared tube reinforced sandwich panel,” *Energy Build.*, vol. 211, p. 109790, 2020, doi: https://doi.org/10.1016/j.enbuild.2020.109790.

[43] R. Moradi-Dastjerdi and K. Behdinan, “Temperature effect on free vibration response of a smart multifunctional sandwich plate,” *J. Sandw. Struct. Mater.*, vol. 23, no. 6, pp. 2399–2421, 2021, doi: 10.1177/1099636220908707.

[44] L. Zhang, F. Zhang, Z. Qin, Q. Han, T. Wang, and F. Chu, “Piezoelectric energy harvester for rolling bearings with capability of self-powered condition monitoring,” *Energy*, vol. 238, p. 121770, 2022, doi: 10.1016/j.energy.2021.121770.

[45] W. Zhao, Z. Liu, G. Yu, and L. Wu, “A new multifunctional carbon fiber honeycomb sandwich structure with excellent mechanical and thermal performances,” *Compos. Struct.*, vol. 274, p. 114306, 2021, doi: https://doi.org/10.1016/j.compstruct.2021.114306.

[46] B. Safaei, P. Naseradinmousavi, and A. Rahmani, “Development of an accurate molecular mechanics model for buckling behavior of multi-walled carbon nanotubes under axial compression,” *J. Mol. Graph. Model.*, vol. 65, pp. 43–60, 2016, doi: 10.1016/j.jmgm.2016.02.001.

[47] Y. Chen, L. Zhang, C. He, R. He, B. Xu, and Y. Li, “Thermal insulation performance and heat transfer mechanism of C/SiC corrugated lattice core sandwich panel,” *Aerosp. Sci. Technol.*, vol. 111, p. 106539, 2021, doi: 10.1016/j.ast.2021.106539.

[48] B. Safaei, R. Moradi-Dastjerdi, K. Behdinan, Z. Qin, and F. Chu, “Thermoelastic behavior of sandwich plates with porous polymeric core and

CNT clusters/polymer nanocomposite layers," *Compos. Struct.*, vol. 226, p. 111209, 2019, doi: https://doi.org/10.1016/j.compstruct.2019.111209.

[49] M. Asmael, B. Safaei, Q. Zeeshan, O. Zargar, and A. A. Nuhu, *Ultrasonic machining of carbon fiber–reinforced plastic composites: a review*, vol. 113, no. 11–12. The International Journal of Advanced Manufacturing Technology, 2021.

[50] S. Rupani, S. Jani, and D. Acharya, "Design, Modelling and Manufacturing aspects of Honeycomb Sandwich Structures: A Review," *Int. J. Sci. Eng. Dev. Res.*, vol. 2, pp. 526–532, Apr. 2017, doi: 10.1712/ijsdr.17013.

[51] Z. Li, Q. Yang, R. Fang, W. Chen, and H. Hao, "Crushing performances of Kirigami modified honeycomb structure in three axial directions," *Thin-Walled Struct.*, vol. 160, p. 107365, 2021, doi: https://doi.org/10.1016/j.tws.2020.107365.

[52] A. Kumar, S. Angra, and A. K. Chanda, "Analysis of the effects of varying core thicknesses of Kevlar Honeycomb sandwich structures under different regimes of testing," *Mater. Today Proc.*, vol. 21, pp. 1615–1623, 2020, doi: https://doi.org/10.1016/j.matpr.2019.11.242.

[53] M. Alhijazi, B. Safaei, Q. Zeeshan, and M. Asmael, "Modeling and simulation of the elastic properties of natural fiber-reinforced thermosets," *Polym. Compos.*, vol. 42, no. 7, pp. 3508–3517, Jul. 2021, doi: https://doi.org/10.1002/pc.26075.

[54] Y. Zhang, Y. Li, K. Guo, and L. Zhu, “Dynamic mechanical behaviour and energy absorption of aluminium honeycomb sandwich panels under repeated impact loads,” *Ocean Eng.*, vol. 219, p. 108344, 2021.

[55] N. Z. M. Zaid, M. R. M. Rejab, and N. A. N. Mohamed, “Sandwich structure based on corrugated-core: a review,” in *MATEC Web of Conferences*, 2016, vol. 74, p. 29.

[56] P. V Katariya, S. K. Panda, and K. Mehar, “Theoretical modelling and experimental verification of modal responses of skewed laminated sandwich structure with epoxy-filled softcore,” *Eng. Struct.*, vol. 228, p. 111509, 2021.

[57] C. Kılıçaslan, *Experimental and Numerical Investigation of the Quasi-Static and High Strain Rate Crushing Behavior of Single and Multi-Layer Zig-Zag 1050 H14 Al Trapezoidal Corrugated Core Sandwich Structures*. Izmir Institute of Technology (Turkey), 2014.

[58] Z. Wang, H. Tian, Z. Lu, and W. Zhou, “High-speed axial impact of aluminum honeycomb - Experiments and simulations,” *Compos. Part B Eng.*, vol. 56, pp. 1–8, 2014, doi: 10.1016/j.compositesb.2013.07.013.

[59] J. Liu, J. Tao, F. Li, and Z. Zhao, “Flexural properties of a novel foam core sandwich structure reinforced by stiffeners,” *Constr. Build. Mater.*, vol. 235, p. 117475, 2020, doi: 10.1016/j.conbuildmat.2019.117475.

[60] T. Li and L. Wang, “Bending behavior of sandwich composite structures with

tunable 3D-printed core materials," *Compos. Struct.*, vol. 175, pp. 46–57, 2017, doi: https://doi.org/10.1016/j.compstruct.2017.05.001.

[61] Y. Wang, V. Ermilov, S. Strigin, and B. Safaei, "Multilevel modeling of the mechanical properties of graphene nanocomposites/polymer composites," *Microsyst. Technol.*, vol. 27, no. 12, pp. 4241–4251, 2021, doi: 10.1007/s00542-021-05218-z.

[62] A. Chemami, K. Bey, J. Gilgert, and Z. Azari, "Behaviour of composite sandwich foam-laminated glass/epoxy under solicitation static and fatigue," *Compos. Part B Eng.*, vol. 43, no. 3, pp. 1178–1184, 2012, doi: https://doi.org/10.1016/j.compositesb.2011.11.051.

[63] I. Barbaros, Y. Yang, B. Safaei, Z. Yang, Z. Qin, and M. Asmael, "State-of-the-art review of fabrication, application, and mechanical properties of functionally graded porous nanocomposite materials," *Nanotechnol. Rev.*, vol. 11, no. 1, pp. 321–371, 2022, doi: 10.1515/ntrev-2022-0017.

[64] X. Li, W. Liu, H. Fang, R. Huo, and P. Wu, "Flexural creep behavior and life prediction of GFRP-balsa sandwich beams," *Compos. Struct.*, vol. 224, p. 111009, 2019, doi: https://doi.org/10.1016/j.compstruct.2019.111009.

[65] P. Ghanati and B. Safaei, "Elastic buckling analysis of polygonal thin sheets under compression," *Indian J. Phys.*, vol. 93, no. 1, pp. 47–52, 2019, doi: 10.1007/s12648-018-1254-9.

[66] L. E. Ribeiro Faria, G. F. Gomes, S. R. G. de Sousa, A. J. Faria Bombard, and A. C. Ancelotti Jr., "Dynamic experimental behavior of sandwich beams with honeycomb core filled with magnetic rheological gel: A statistical approach," *Smart Mater. Struct.*, vol. 29, no. 11, 2020, doi: 10.1088/1361-665X/abb8e7.

[67] P. V. Katariya and S. K. Panda, "Numerical evaluation of transient deflection and frequency responses of sandwich shell structure using higher order theory and different mechanical loadings," *Eng. Comput.*, vol. 35, no. 3, pp. 1009–1026, 2019, doi: 10.1007/s00366-018-0646-y.

[68] J. Fazilati and M. Alisadeghi, "Multiobjective crashworthiness optimization of multi-layer honeycomb energy absorber panels under axial impact," *Thin-Walled Struct.*, vol. 107, pp. 197–206, 2016, doi: 10.1016/j.tws.2016.06.008.

[69] G. X. Ha, D. Marinkovic, and M. W. Zehn, "Parametric investigations of mechanical properties of nap-core sandwich composites," *Compos. Part B Eng.*, vol. 161, pp. 427–438, 2019.

[70] C. Lu *et al.*, "Stress Distribution on Composite Honeycomb Sandwich Structure Suffered from Bending Load," *Procedia Eng.*, vol. 99, pp. 405–412, 2015, doi: 10.1016/j.proeng.2014.12.554.

[71] A. Sakly, A. Laksimi, H. Kebir, and S. Benmedakhen, "Experimental and modelling study of low velocity impacts on composite sandwich structures for railway applications," *Eng. Fail. Anal.*, vol. 68, pp. 22–31, 2016, doi: 10.1016/j.engfailanal.2016.03.001.

[72] B. Sahoo, K. Mehar, B. Sahoo, N. Sharma, and S. K. Panda, “Thermal frequency analysis of FG sandwich structure under variable temperature loading TT -,” *Struct. Eng. Mech. An Int ′l J.*, vol. 77, pp. 57–74, 2021, [Online]. Available: http://www.dbpia.co.kr/journal/articleDetail?nodeId=NODE10696843.

[73] W. He, J. Liu, B. Tao, D. Xie, J. Liu, and M. Zhang, “Experimental and numerical research on the low velocity impact behavior of hybrid corrugated core sandwich structures,” *Compos. Struct.*, vol. 158, pp. 30–43, 2016, doi: 10.1016/j.compstruct.2016.09.009.

[74] Q. Han *et al.*, “Experimental investigation on impact and bending properties of a novel dactyl-inspired sandwich honeycomb with carbon fiber,” *Constr. Build. Mater.*, vol. 253, p. 119161, 2020, doi: 10.1016/j.conbuildmat.2020.119161.

[75] C. Peng, K. Fox, M. Qian, H. Nguyen-Xuan, and P. Tran, “3D printed sandwich beams with bioinspired cores: Mechanical performance and modelling,” *Thin-Walled Struct.*, vol. 161, p. 107471, 2021, doi: https://doi.org/10.1016/j.tws.2021.107471.

[76] D. Harland, A. W. Alshaer, and H. Brooks, “An Experimental and Numerical Investigation of a Novel 3D Printed Sandwich Material for Motorsport Applications,” *Procedia Manuf.*, vol. 36, pp. 11–18, 2019, doi: https://doi.org/10.1016/j.promfg.2019.08.003.

[77] K. Sugiyama, R. Matsuzaki, M. Ueda, A. Todoroki, and Y. Hirano, “3D printing

of composite sandwich structures using continuous carbon fiber and fiber tension," *Compos. Part A Appl. Sci. Manuf.*, vol. 113, pp. 114–121, 2018, doi: https://doi.org/10.1016/j.compositesa.2018.07.029.

[78] Z. Li, Q. Yang, W. Chen, H. Hao, R. Fang, and J. Cui, "Dynamic compressive properties of reinforced and kirigami modified honeycomb in three axial directions," *Thin-Walled Struct.*, vol. 171, no. December 2021, p. 108692, 2022, doi: 10.1016/j.tws.2021.108692.

[79] J. Aboudi, S. M. Arnold, and B. A. Bednarcyk, *Micromechanics of composite materials: a generalized multiscale analysis approach*. Butterworth-Heinemann, 2013.

[80] S. Bargmann *et al.*, "Generation of 3D representative volume elements for heterogeneous materials: A review," *Prog. Mater. Sci.*, vol. 96, pp. 322–384, 2018, doi: 10.1016/j.pmatsci.2018.02.003.

[81] K. P. Babu, P. M. Mohite, and C. S. Upadhyay, "Development of an RVE and its stiffness predictions based on mathematical homogenization theory for short fibre composites," *Int. J. Solids Struct.*, vol. 130–131, pp. 80–104, 2018, doi: 10.1016/j.ijsolstr.2017.10.011.

[82] S. Sorohan, D. M. Constantinescu, M. Sandu, and A. G. Sandu, "In-plane homogenization of commercial hexagonal honeycombs considering the cell wall curvature and adhesive layer influence," *Int. J. Solids Struct.*, vol. 156–157, pp. 87–106, 2019, doi: 10.1016/j.ijsolstr.2018.08.007.

[83] B. Safaei, A. M. Fattahi, and F. Chu, “Finite element study on elastic transition in platelet reinforced composites,” *Microsyst. Technol.*, vol. 24, no. 6, pp. 2663–2671, 2018, doi: 10.1007/s00542-017-3651-y.

[84] C. Qiu, Z. Guan, S. Jiang, and Z. Li, “A method of determining effective elastic properties of honeycomb cores based on equal strain energy,” *Chinese J. Aeronaut.*, vol. 30, no. 2, pp. 766–779, 2017, doi: 10.1016/j.cja.2017.02.016.

[85] L. Wahl, S. Maas, D. Waldmann, A. Zürbes, and P. Frères, “Shear stresses in honeycomb sandwich plates: Analytical solution, finite element method and experimental verification,” *J. Sandw. Struct. Mater.*, vol. 14, no. 4, pp. 449–468, 2012, doi: 10.1177/1099636212444655.

[86] N. Ahmed, N. Zafar, and H. Z. Janjua, “Homogenization of Honeycomb Core in Sandwich Structures: A Review,” *Proc. 2019 16th Int. Bhurban Conf. Appl. Sci. Technol. IBCAST 2019*, pp. 159–173, 2019, doi: 10.1109/IBCAST.2019.8667144.

[87] D. Harland, A. W. Alshaer, and H. Brooks, “An experimental and numerical investigation of a novel 3D printed sandwich material for motorsport applications,” *Procedia Manuf.*, vol. 36, pp. 11–18, 2019, doi: 10.1016/j.promfg.2019.08.003.

[88] D. Xiao, X. Chen, Y. Li, W. Wu, and D. Fang, “The structure response of sandwich beams with metallic auxetic honeycomb cores under localized impulsive loading-experiments and finite element analysis,” *Mater. Des.*, vol.

176, p. 107840, 2019, doi: 10.1016/j.matdes.2019.107840.

[89] R. Kumar and S. Patel, “Failure analysis on octagonal honeycomb sandwich panel under air blast loading,” *Mater. Today Proc.*, vol. 46, pp. 9667–9672, 2019, doi: 10.1016/j.matpr.2020.07.525.

[90] R. Adams, S. Townsend, S. Soe, and P. Theobald, “Finite element-based optimisation of an elastomeric honeycomb for impact mitigation in helmet liners,” *Int. J. Mech. Sci.*, vol. 214, no. August 2021, p. 106920, 2022, doi: 10.1016/j.ijmecsci.2021.106920.

[91] J. Naveen, M. Jawaid, A. Vasanthanathan, and M. Chandrasekar, “9 - Finite element analysis of natural fiber-reinforced polymer composites,” in *Woodhead Publishing Series in Composites Science and Engineering*, M. Jawaid, M. Thariq, and N. B. T.-M. of D. P. in B. Saba Fibre-Reinforced Composites and Hybrid Composites, Eds. Woodhead Publishing, 2019, pp. 153–170.

[92] S. Xie, H. Wang, C. Yang, H. Zhou, and Z. Feng, “Mechanical properties of combined structures of stacked multilayer Nomex® honeycombs,” *Thin-Walled Struct.*, vol. 151, no. February, p. 106729, 2020, doi: 10.1016/j.tws.2020.106729.

[93] P. S. Krishna, A. Mohan, P. U. Ahamed, and S. P. Jani, “Materials Today : Proceedings Bending analysis of honeycomb sandwich panels with metallic face sheets and GFRP core,” *Mater. Today Proc.*, no. xxxx, 2022, doi: 10.1016/j.matpr.2021.12.050.

[94] N. V Nguyen, H. Nguyen-Xuan, T. N. Nguyen, J. Kang, and J. Lee, “A comprehensive analysis of auxetic honeycomb sandwich plates with graphene nanoplatelets reinforcement,” *Compos. Struct.*, vol. 259, p. 113213, 2021, doi: https://doi.org/10.1016/j.compstruct.2020.113213.

[95] E. Kadum Njim, S. H. Bakhy, and M. Al-Waily, “Analytical and numerical investigation of buckling load of functionally graded materials with porous metal of sandwich plate,” *Mater. Today Proc.*, 2021, doi: https://doi.org/10.1016/j.matpr.2021.03.557.

[96] U. K. Kar and J. Srinivas, “Material modeling and analysis of hydroxyapatite/titanium FGM plate under thermo-mechanical loading conditions,” *Mater. Today Proc.*, vol. 33, pp. 5498–5504, 2020, doi: 10.1016/j.matpr.2020.03.312.

[97] B. Meyghani, M. B. Awang, S. S. Emamian, M. K. B. Mohd Nor, and S. R. Pedapati, “A comparison of different finite element methods in the thermal analysis of friction stir welding (FSW),” *Metals (Basel).*, vol. 7, no. 10, p. 450, 2017.

[98] A. Atiqah, M. N. M. Ansari, and L. Premkumar, “Impact and hardness properties of honeycomb natural fibre reinforced epoxy composites,” *Mater. Today Proc.*, vol. 29, no. November 2018, pp. 138–142, 2019, doi: 10.1016/j.matpr.2020.05.645.

[99] X. Dai, T. Yuan, Z. Zu, H. Ye, X. Cheng, and F. Yang, “Experimental

investigation on the response and residual compressive property of honeycomb sandwich structures under single and repeated low velocity impacts," *Mater. Today Commun.*, vol. 25, no. March, p. 101309, 2020, doi: 10.1016/j.mtcomm.2020.101309.

[100] R. Yogeswaran and P. Pitchipoo, "Characterization and machining analysis of AA3003 honeycomb sandwich," *Mater. Today Proc.*, vol. 28, pp. 4–7, 2020, doi: 10.1016/j.matpr.2019.12.101.

[101] C. Yang, P. Xu, S. Yao, S. Xie, Q. Li, and Y. Peng, "Optimization of honeycomb strength assignment for a composite energy-absorbing structure," *Thin-Walled Struct.*, vol. 127, no. March, pp. 741–755, 2018, doi: 10.1016/j.tws.2018.03.014.

[102] J. R. Dutra, S. L. Moni Ribeiro Filho, A. L. Christoforo, T. H. Panzera, and F. Scarpa, "Investigations on sustainable honeycomb sandwich panels containing eucalyptus sawdust, Piassava and cement particles," *Thin-Walled Struct.*, vol. 143, no. May, p. 106191, 2019, doi: 10.1016/j.tws.2019.106191.

[103] B. Vijaya Ramnath, C. Elanchezhian, V. M. Manickavasagam, R. Surya Narayanan, R. Sudharshan, and G. Pugazhendhi, "A review on sandwich composites and their advancements," *Mater. Today Proc.*, vol. 16, pp. 1146–1151, 2019, doi: 10.1016/j.matpr.2019.05.207.

[104] O. Thomsen, "Sandwich Materials for Wind Turbine Blades -- Present and Future," *J. Sandw. Struct. Mater. - J SANDW STRUCT MATER*, vol. 11, pp. 7–

26, Jan. 2009, doi: 10.1177/1099636208099710.

[105] R. D. Pham and G. Hütter, “Influence of topology and porosity on size effects in stripes of cellular material with honeycomb structure under shear, tension and bending,” *Mech. Mater.*, vol. 154, p. 103727, 2021.

[106] H. G. Allen, *Analysis and design of structural sandwich panels: the commonwealth and international library: structures and solid body mechanics division*. Elsevier, 2013.

[107] J.-J. R. B. Bekuit, D. C. D. Oguamanam, and O. Damisa, “A quasi-2D finite element formulation for the analysis of sandwich beams,” *Finite Elem. Anal. Des.*, vol. 43, no. 14, pp. 1099–1107, 2007, doi: https://doi.org/10.1016/j.finel.2007.08.005.

[108] S. Lecturer, “Front Matter,” *Anal. Des. Struct. Sandw. Panels*, p. iii, 1969, doi: 10.1016/b978-0-08-012870-2.50001-8.

[109] N. A. Fleck and I. Sridhar, “End compression of sandwich columns,” *Compos. - Part A Appl. Sci. Manuf.*, vol. 33, no. 3, pp. 353–359, 2002, doi: 10.1016/S1359-835X(01)00118-X.

[110] M. Aslan, O. Güler, K. Çava, Ü. Alver, and E. Yüceloğlu, *An Investigation on the Mechanical Properties of the Sandwich Panel Composites*. 2017.

[111] R. Potluri, A. Eswara Kumar, M. Naga Raju, and K. R. P. Babu, “Finite Element

Analysis ofCellular Foam Core Sandwich Structures," *Mater. Today Proc.*, vol. 4, no. 2, pp. 2501–2510, 2017, doi: 10.1016/j.matpr.2017.02.103.

[112] A. Boudjemai, R. Amri, A. Mankour, H. Salem, M. H. Bouanane, and D. Boutchicha, "Modal analysis and testing of hexagonal honeycomb plates used for satellite structural design," *Mater. Des.*, vol. 35, pp. 266–275, 2012, doi: 10.1016/j.matdes.2011.09.012.

[113] S. Upreti, V. K. Singh, S. K. Kamal, A. Jain, and A. Dixit, "Modelling and analysis of honeycomb sandwich structure using finite element method," *Mater. Today Proc.*, vol. 25, pp. 620–625, 2020, doi: https://doi.org/10.1016/j.matpr.2019.07.377.

[114] H. Rahman, R. Jamshed, H. Hameed, and S. Raza, "Finite element analysis (FEA) of honeycomb sandwich panel for continuum properties evaluation and core height influence on the dynamic behavior," *Adv. Mater. Res.*, vol. 326, pp. 1–10, 2011, doi: 10.4028/www.scientific.net/AMR.326.1.

[115] T. Ogasawara, S. Ayabe, Y. Ishida, T. Aoki, and Y. Kubota, "Heat-resistant sandwich structure with carbon fiber-polyimide composite faces and a carbon foam core," *Compos. Part A Appl. Sci. Manuf.*, vol. 114, no. August, pp. 352–359, 2018, doi: 10.1016/j.compositesa.2018.08.030.

[116] P. Goswami, M. E. Student, R. Indore, and M. Pradesh, "Thermal Insulation analysis of an Aramid honeycomb Sandwich Structure Filled with Silica Aerogel," vol. 3, no. 7, pp. 1–6, 2018.